

**Modeling of a
Turbo Charged Spark Ignited Engine
LiTH-ISY-EX-2081**

Examensarbete utfört i Fordonssystem
vid Tekniska Högskolan i Linköping
av

Johan Bergström & Jan Brugård

Reg nr: LiTH-ISY-EX-2081

**Modeling of a
Turbo Charged Spark Ignited Engine
LiTH-ISY-EX-2081**

Examensarbete utfört i Fordonssystem
vid Tekniska Högskolan i Linköping
av

Johan Bergström & Jan Brugård

Reg nr: LiTH-ISY-EX-2081

Supervisor: **Lars Eriksson**
David Holmgren

Examiner: **Lars Nielsen**

Linköping, October 26, 1999.

	Avdelning, Institution Division, Department Vehicular Systems Dept. of Electrical Engineering	Datum: Date: 1999-10-26		
	<table border="1"> <tr> <td> Språk Language <input type="checkbox"/> Svenska/Swedish <input checked="" type="checkbox"/> Engelska/English <input type="checkbox"/> _____ </td> <td> Rapporttyp Report category <input type="checkbox"/> Licentiatavhandling <input checked="" type="checkbox"/> Examensarbete <input type="checkbox"/> C-uppsats <input type="checkbox"/> D-uppsats <input type="checkbox"/> Övrig rapport <input type="checkbox"/> _____ </td> <td> ISBN ISRN Serietitel och serienummer ISSN Title of series, numbering _____ LiTH-ISY-EX-2081 </td> </tr> </table>	Språk Language <input type="checkbox"/> Svenska/Swedish <input checked="" type="checkbox"/> Engelska/English <input type="checkbox"/> _____	Rapporttyp Report category <input type="checkbox"/> Licentiatavhandling <input checked="" type="checkbox"/> Examensarbete <input type="checkbox"/> C-uppsats <input type="checkbox"/> D-uppsats <input type="checkbox"/> Övrig rapport <input type="checkbox"/> _____	ISBN ISRN Serietitel och serienummer ISSN Title of series, numbering _____ LiTH-ISY-EX-2081
Språk Language <input type="checkbox"/> Svenska/Swedish <input checked="" type="checkbox"/> Engelska/English <input type="checkbox"/> _____	Rapporttyp Report category <input type="checkbox"/> Licentiatavhandling <input checked="" type="checkbox"/> Examensarbete <input type="checkbox"/> C-uppsats <input type="checkbox"/> D-uppsats <input type="checkbox"/> Övrig rapport <input type="checkbox"/> _____	ISBN ISRN Serietitel och serienummer ISSN Title of series, numbering _____ LiTH-ISY-EX-2081		
Titel: Modellering av en bensindriven turbomotor Title: Modeling of a Turbo Charged Spark Ignited Engine Författare: Johan Bergström & Jan Brugård Author:				
Sammanfattning Abstract <p>För diagnos och vid utveckling av nya regulatorer till en turbomotor är det önskvärt att ha en simuleringsmodell som täcker alla motorns delsystem. En medelvärdesmodell för en bensindriven 2.3 liters SAAB turbomotor har tagits fram. Tonvikten ligger på att modellera tryck, temperaturer och massflöden för luftfilter, trottell, insugningsrör, cylindrar, kompressor och turbin.</p> <p>För att erhålla modeller som är så generella som möjligt är de flesta av dem baserade på välkända fysikaliska samband, men när detta inte har varit möjligt eller visat sig otillräckligt har "black-box"-modeller använts. De flesta av modellerna som tagits fram är rent statiska, d.v.s. de har beräknats utgående från mätdata som erhållits från experiment där motorns arbetspunkt hållits konstant tills alla parametrar av intresse nått stationärt tillstånd. De dynamiska delar som studerats innefattar insugningsröret och turboaggregatet.</p> <p>De presenterade modellerna ger insikt i motorns uppförande och förslag till möjliga förbättringar och utvidgningar ges också.</p>				
Nyckelord Keywords MVEM, simulation, efficiency, pressure, temperature, engine speed				

Abstract

For diagnosis purposes and in order to develop new controllers for Spark Ignited (SI) turbo engines, it is desirable to have complete simulation models that covers all subsystems. A Mean Value Engine Model (MVEM) for a SAAB 2.3 litres SI Turbo Charged engine is developed, emphasizing on pressures, temperatures and mass flows for the air filter, intercooler, throttle, manifolds, cylinders, compressor and turbine.

To get models that are as general as possible, they are in most cases based on well known physical relationships, but when this approach fails or is insufficient, black or grey box models are used. Most of the models presented are purely static, i.e. they are calculated from data that is obtained from experiments where the working condition is kept constant until stationary conditions are achieved. The dynamics considered includes models for the intake manifold and the turbo shaft speed.

The presented models gives insight into the behavior of the engine and suggestions for future improvements are also given.

Acknowledgements

This work has been carried out at the division of Vehicular Systems, Linköping University, in cooperation with SAAB Automobile, with Lars Eriksson and David Holmgren as supervisors. We would like to thank Lars Eriksson and our examiner Lars Nielsen for leading us into the area of mean value engine modeling. We would also like to thank them for supplying us with figures 2.1, 2.2, 2.3 and 5.1. We would also like to thank SAAB Automobile for providing experimental equipment and support for the experiments. Especially we would like to thank David Holmgren at SAAB Automobile.

For the experimental part, our reasearch engineer Andrej Perkovic is acknowledged for help with experiments. Finally Per Andersson is gratefully acknowlged for many insightful discissions and help at the lab.

Linköping, October 1999

Johan Bergström and Jan Brugård

Nomenclature

<i>Symbol</i>	Quantity (explanation)	unit
(A/F)	Air-to-fuel ratio	-
D_2	impeller tip diameter for compressor	m
$D_{2,t}$	impeller tip diameter for turbine	m
\dot{m}_{air}	Intake air mass flow rate	kg/h
$\dot{m}_{air,c}$	Intake air mass flow rate into cylinders	kg/h
\dot{m}_{cool}	Cooling air mass flow rate	kg/h
\dot{m}_{exh}	Exhaust manifold gas mass flow rate	kg/h
$\dot{m}_{exh,c}$	Exhaust gas mass flow rate out from cylinders	kg/h
\dot{m}_{fuel}	Fuel mass flow	kg/h
$\dot{m}_{turbine}$	Turbine exhaust gas mass flow rate	kg/h
\dot{m}_{wg1}	Exhaust gas mass flow rate into turbine	kg/h
\dot{m}_{wg2}	Exhaust gas mass flow rate directly to catalyst	kg/h
N	Engine speed	rpm
N_t	Turbo shaft speed	rpm
p_{amb}	Ambient pressure	kPa
p_{af}	Air filter outlet pressure	kPa
p_{comp}	Compressor outlet pressure	kPa
p_{exh}	Exhaust manifold pressure	kPa
p_{int}	Intercooler outlet pressure	kPa
p_{man}	Intake manifold pressure	kPa
p_{th}	Throttle plate outlet pressure	kPa
$p_{turbine}$	Turbine outlet pressure	kPa
p_r	Ratio of outlet and inlet pressure, general case	-
$p_{r,af}$	Ratio of air filter outlet and inlet pressure	-
$p_{r,c}$	Ratio of compressor outlet and inlet pressure	-
$p_{r,i}$	Ratio of intercooler outlet and inlet pressure	-
$p_{r,t}$	Ratio of turbine outlet and inlet pressure	-
$p_{r,th}$	Ratio of throttle outlet and inlet pressure	-
t_{inj}	Fuel injection time	ms
T	Engine torque	Nm
T_{amb}	Ambient temperature	K
T_{af}	Air filter outlet air temperature	K
T_{comp}	Compressor outlet air temperature	K
T_{exh}	Engine outlet air temperature	K
T_{int}	Intercooler outlet air temperature	K
T_{cool}	Intercooler cooling air temperature	K
$T_{turbine}$	Turbine outlet air temperature	K
V_d	Total cylinder displacement volume	l
V_{man}	Intake manifold volume	l

<i>Symbol</i>	Quantity (explanation)	unit
α	Throttle plate angle	rad
ε	Intercooler efficiency	-
γ	Ratio of specific heats c_p/c_v	-
λ	Normalized (A/F)	-
η_c	Compressor isentropic efficiency	-
η_t	Turbine isentropic efficiency	-

Abbreviations

SI	Spark Ignited
MVEM	Mean Value Engine Model
TDC	Top Dead Center
BDC	Bottom Dead Center
ATDC	After TDC
BTDC	Before TDC
MEP	Mean Effective Pressure

Contents

1	Introduction	15
1.1	Problem Specification and Objective	15
1.2	Methods	16
1.3	Disposition	16
1.4	Related Work	17
2	SI Engine Modeling	19
2.1	Engine System	19
2.2	Four Stroke Cycle	20
2.3	Model Overview	21
2.3.1	Experimental Procedures	22
3	Intake System	25
3.1	Air Filter	26
3.1.1	Air Filter Measurement Procedures	26
3.1.2	Pressure Models	26
3.1.3	Air Filter Summary	29
3.2	Intercooler	30
3.2.1	Intercooler Measurement Procedures	31
3.2.2	Temperature Models	33
3.2.3	Pressure Models	37
3.2.4	Intercooler Summary	40
3.3	Throttle	41
3.3.1	Throttle Measurement Procedures	41

3.3.2	Air Mass Flow Model	41
3.3.3	Throttle Summary	44
3.4	Intake System Dynamics	45
3.4.1	Pressure Dynamics	45
3.4.2	Temperature Dynamics	47
3.4.3	Intake Manifold Summary	49
4	Turbo	51
4.1	Compressor Nomenclature	52
4.2	Compressor	53
4.2.1	Compressor Geometry	53
4.2.2	Physical Relationships for Compressor	54
4.2.3	Compressor Measurement Procedures	56
4.2.4	Pressure Model	58
4.2.5	Efficiency Model	61
4.2.6	Compressor Summary	63
4.3	Turbine	64
4.3.1	Physical Relationships for the Turbine	64
4.3.2	Turbine Measurement Procedures	64
4.3.3	Turbine Isentropic Efficiency Model	65
4.3.4	Pressure Model	65
4.3.5	Turbine Summary	67
4.4	Turbo Dynamics	68
4.4.1	Turbine Shaft Speed	68
4.4.2	Turbine Shaft Speed Summary	70
5	Engine	71
5.1	Fuel Dynamics	72
5.1.1	Fuel Injection	72
5.1.2	Wall Wetting	73
5.1.3	Fuel Dynamics Summary	74
5.2	Engine Torque	75
5.3	Engine Inertia	75
6	Summary	77
6.1	Conclusions	77
6.2	Future Work	77
A	The System	83
B	Theory	85
B.1	Multiple Linear Regression	86
B.2	Thermodynamics	88
B.2.1	Steady Flow System	89
B.2.2	Applied Thermodynamics for MVEM	89
B.2.3	Thermodynamic Properties	90

Chapter 1

Introduction

1.1 Problem Specification and Objective

In the development stage of regulators, different models of the system for regulator design and validation are used. To perform tests and evaluations of different strategies for regulation it is desirable to have a complete simulation model for the studied device, in this case a Spark Ignited (SI) turbo charged engine. To capture the main effects that influence the control design of a turbo charged SI engine, Mean Value Engine Models (MVEM) are used. For MVEM's the considered parameters are averaged over one or several engine cycles, that is the cycle by cycle variations are not considered. Furthermore, processes which establish equilibrium within the course of one or a few engine cycles are considered to be *instantaneous*. They are expressed as algebraic equations, i.e. with no time dependence involved. Processes that reach equilibrium within a few to 1000 engine cycles are referred to as *time developing* relationships and are expressed by differential equations. The objective of this project is to develop an MVEM for the SAAB 2.3 liter turbo charged engine in Vehicular Systems laboratory, and the following sub goals were stated:

- Evaluate existing MVEMs for all subsystems of a turbo charged spark ignited engine.
- Construct a mean value model that is purely static, i.e. the model is built from data that is obtained from experiments where the working condition is held constant until stationary conditions are achieved.
- Investigate how well this static model captures the engine behavior under dynamic engine operation.

- Identify which parts of the model that can not describe the performance satisfactory and explain why.
- Extend the model with required dynamic models (if time available).

1.2 Methods

For each subsystem a physical model is derived based on the laws of thermodynamics, fluid mechanics, Newton's laws, etc. Using the physics and making reasonable simplifications, e.g. assuming ideal gas or that the specific heat is constant in a certain range of the temperature, models are developed. Sometimes there are still parameters that are not known or easily measured. To develop the final model in these cases, different approaches are taken. For the static models, the most common method in this text is to use correlation analysis to investigate which variables influence the parameter of interest and then chose appropriate combinations of the input signals as regressors in a linear, or in some cases, a non linear regression model. The coefficients in this model are then calculated by a least squares fit to data obtained from measurements in the engine test-bench at Vehicular Systems laboratory or, for the turbo charger, from data supplied by the manufacturer. Finally the model is validated for a set of data that was not used calculating the model.

In order to identify the parts of the engine that need to be modeled as a dynamic relation, i.e with a differential equation, the step response of the output signal were studied. The actual equation is then derived from a balance equation that expresses the conservation of some property e.g mass, and unknown parameters are tuned to correspond with measurements.

1.3 Disposition

A description of how an SI engine works and a model overview is given in chapter 2. In the following chapters, 3 - 5, each submodel is presented. When reading these chapters it might be a good idea to look back on chapter 2 to get a reminder of the interconnections of the submodels before reading respective section. At the end of each section in these chapters a summary of the submodel is presented. Finally conclusions for the entire thesis are made in chapter 6.

To get a good understanding of how an engine work, basic knowledge about thermodynamic systems and fluid mechanics are needed. A revise of thermodynamics is therefore given in appendix B.2. A short description of multiple linear and non linear regression is also given in appendix B.1 as it is a very helpful tool for model development. Finally, the theory needed in fluid mechanics is presented in connection with the submodel where it is applicable.

1.4 Related Work

The two main textbooks covering Combustion Engine Fundamentals are written by Watson & Janota [13] and Heywood [12]. Both are very comprehensive and certainly recommended, especially as reference manuals. Some of the work done on modeling of turbo charged spark ignited engines is done by Hendricks et al. at the Technical University of Denmark ([15], [16] and [17]), Moraal and Kolmanovsky at Ford([14]), Olin and Maloney at Delphi Automotive Systems ([23]) and by Guzzella and Amstutz at the Swiss Federal Institute of Technology ([24]).

Chapter 2

SI Engine Modeling

The purpose of an automotive engine is to supply the power needed to move the vehicle. This is accomplished by producing mechanical power from the chemical energy contained in the fuel, in this case gasoline. This energy is released by burning or oxidizing the fuel. For *internal* combustion engines this is done inside the engine, where the fuel-air mixture before combustion and the burned products after combustion are the actual working fluids. The work transfer which provides the desired power output occur directly between this working fluids and the mechanical components of the engine. In this thesis a turbo charged SI engine, or Otto engine after Otto, who first developed the SI engine in 1876, is treated. Sometimes SI engines may also be referred to as gasoline or petrol engines, even though other fuels can be used.

2.1 Engine System

A schematic overview of the engine with surrounding devices is given in figure 2.1. The amount of air entering the engine is governed primary by the angle of the throttle. When the air enters the system it first passes an air filter that takes care of some pollutants, such as dust, to protect the engine. After this the air reaches the compressor where pressure is increased, resulting in increased density. A larger amount of air may thus enter the cylinders at each cycle, resulting in higher power output. However, the effect of the pressure increase is partly counteracted by an increase of temperature in the compressor. To decrease the temperature, the air passes through a heat exchanger, the intercooler, before it passes the throttle and enters the intake manifold, which acts as a reservoir to give a steady flow of air

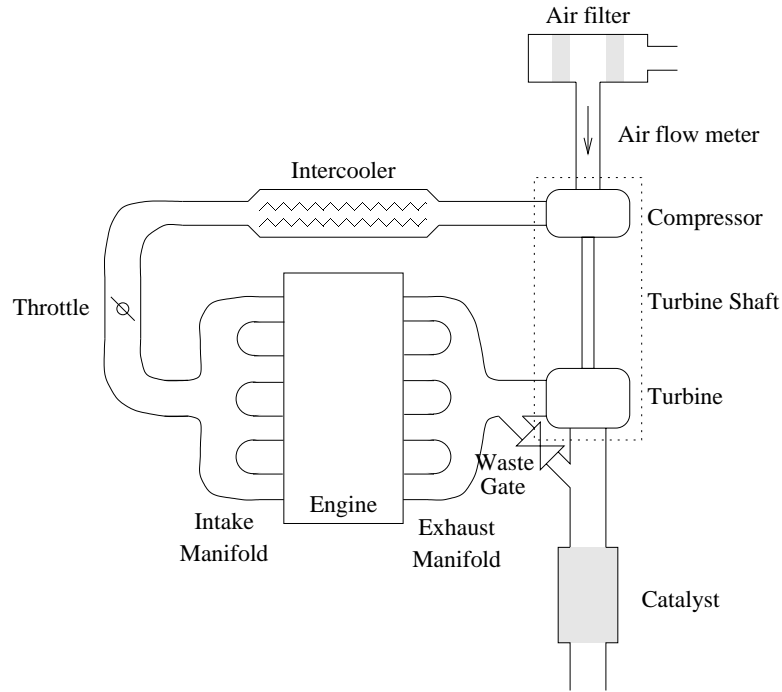


Figure 2.1 Schematic figure of SI engine with turbo charger

into the engine. The actual work is done in the cylinders in a four stroke cycle, described in section 2.2. After the combustion the exhaust gases pass the exhaust manifold and part of it is used to propel the turbine, which delivers power to the compressor. The rest of the exhaust gases are bypassed through a waste gate, used to protect the turbine from overspeeding, but also to control the amount of power delivered to the compressor. All the exhaust gases are then passed through a catalyst and cleaned before it leaves the system.

2.2 Four Stroke Cycle

For a four stroke engine the combustion cycle is divided into four steps, strokes, illustrated in figure 2.2 and described below. Note that all the mentioned values of the crank shaft angle are only examples and may vary a lot from one engine to another.

The first stroke is called the *intake stroke* (from top dead center (TDC) to bottom dead center (BDC)). During this, the intake valve is open and while the piston moves downwards the cylinder is filled with a fresh air/fuel charge from the intake manifold. Due to the open inlet valve the cylinder pressure remains fairly

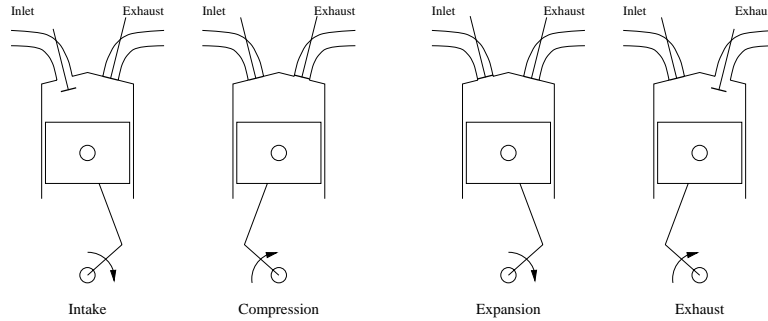


Figure 2.2 The four strokes intake, compression, expansion, and exhaust of a four stroke internal combustion engine.

constant.

A *compression stroke* (BDC-TDC) follows, where the air/fuel mixture is compressed to higher temperatures and pressures through the mechanical work produced by the piston. About 25° BTDC (before TDC) a spark ignites the mixture and initiates the combustion, whereas the flame propagates through the combustion chamber and adds heat to the fluid.

The combustion continues into the *expansion stroke* (TDC-BDC) and finishes around 40° ATDC (after TDC). Work is produced by the fluid during the expansion stroke when the volume expands. Around 130° ATDC the exhaust port is opened and the blowdown process starts, where the cylinder pressure decreases as the fluid is blown out into the exhaust system by the higher pressure in the cylinder.

During the final stroke, *exhaust stroke* (BDC-TDC), the valves are still open and therefore the pressure in the cylinder is close to the pressure in the exhaust system and the rest of the fluid in the combustion chamber is pushed out into the exhaust system as the piston moves upwards. When the piston reaches TDC a new cycle starts with the intake stroke. The described four stroke cycle results in the pressure-volume diagram illustrated in figure 2.3.

2.3 Model Overview

Figure 2.4 shows an overview of the submodels presented in this thesis and their interconnections. When reading about each submodel in the following chapters it might be a good idea to go back to figure 2.4 to see how each submodel interact with the others. Note that input and output signals are not always connected in the order one might think of when looking at the physical connections, illustrated in figure 2.1, e.g. air mass flow is given as an output from the throttle model and taken as an input to most other models. Note that models for the Catalyst, Exhaust Manifold and Waste Gate are not presented in this thesis. They are all left to future projects due to lack of control of the exhaust gas flow at our test bench.

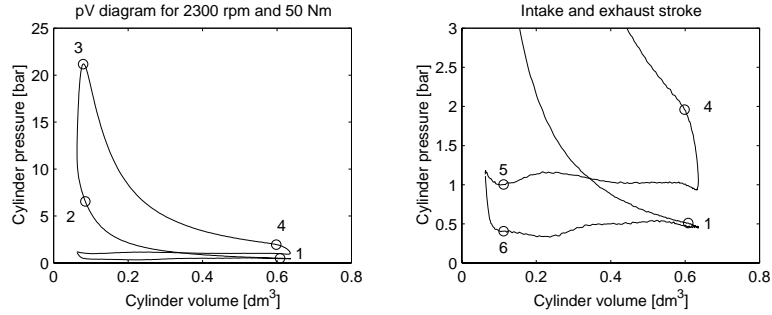


Figure 2.3 *pV* diagram for the four stroke cycle. The left plot shows the full cycle and the right figure shows the intake and exhaust stroke enlarged. The marked points corresponds to: 1) Inlet valve closing. 2) Start of combustion. 3) Maximum pressure. 4) Exhaust valve opening. 5) Inlet valve opening. 6) Exhaust valve closing.

2.3.1 Experimental Procedures

When modeling each subsystem, an analysis of which input and output signals are needed is made. Then experiments are done to get the time needed before the system reaches stationary *operating conditions*, that is constant pressures, temperatures, mass flows, etc., after changing throttle angle or engine speed. When this is done the actual experiment is made by choosing an appropriate span of engine speeds and throttle angles and then running the engine through all these chosen operating conditions. After each change of operating condition the engine is run enough time to reach stationary conditions, input and output parameters are then sampled for a couple of seconds and averaged. The obtained information is then used to develop the models.

The chosen input and output signals for each submodel are given in figure 2.4. Note that inlet and outlet temperatures, T , rather than efficiencies, η , showed as signals in the figure, are measured. These temperatures are then used to calculate the efficiencies.

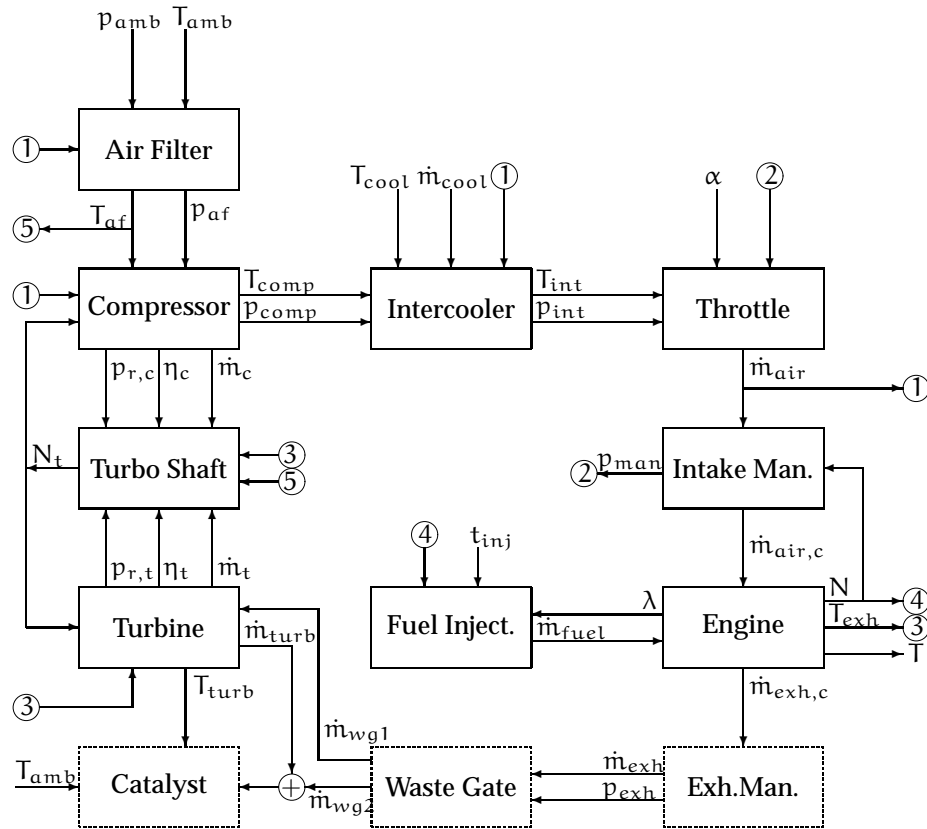


Figure 2.4 Input and output signals from engine subsystems and the interconnection between them. For readability some signals are marked with numbers. An input marked with a number is connected to the output signal marked with the same number.

Chapter 3

Intake System

The Intake System consists of air filter, compressor, intercooler, throttle, and intake manifold. In this chapter models for all parts, except the compressor, are developed. The model for the compressor is presented in section 4.2 in connection with the rest of the turbo charger.

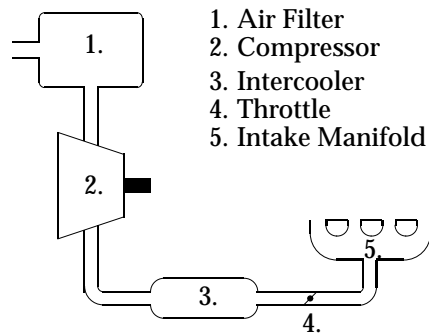


Figure 3.1 Sketch of the intake system.

3.1 Air Filter

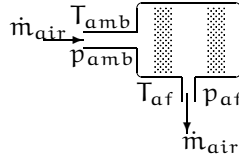


Figure 3.2 Sketch of air filter.

Besides the obvious, and desired, effect of cleaning the air from some pollutants, the air filter also has the effect of lowering the pressure, hence a model for this pressure loss should be made. Also models for the ability of the air filter to take care of e.g. dust particles and moisture (and how this affects the engine) are of interest, but are not considered here.

3.1.1 Air Filter Measurement Procedures

The following experiment was performed on the air filter:

- \dot{m}_{air} , T_{amb} , T_{af} and p_{af} were measured for different engine speeds and throttle plate positions, p_{amb} was estimated to be constant and equal to the maximum value of p_{af} , that is air filter outlet pressure when there is no flow.
- N ranges from 1500 rpm to 4500 rpm with steps of 500 rpm.
- α is varied in the entire engine working area.
- The parameters of interest were measured during 3 seconds and then averaged after waiting 10 seconds between each change in operating condition for stabilization of pressure and temperatures.

3.1.2 Pressure Models

When liquid flows through a tube there is normally a loss of power through friction against the walls and internal friction in the fluid. This leads to a pressure drop over the tube. The pressure drop depends on the volumetric flow, Q (volume per time unit), and generally we can write

$$p(t) = h_1(Q(t))$$

The properties of the function h_1 depends on the properties of the tube. If the tube is thin or filled with a porous medium, d'Arcy's law applies¹:

$$p(t) = R_f Q(t) \tag{3.1}$$

¹d'Arcy's law is named after Henry d'Arcy (1803-1858), recognized as the father of groundwater hydraulics.

correlation	\dot{m}_{air}	\dot{m}_{air}^2	$T_{\text{amb}}\dot{m}_{\text{air}}^2$	$T_{\text{amb}}^2\dot{m}_{\text{air}}^2$
p_{loss}	0.9618	0.9991	0.9992	0.9992

Figure 3.3 Correlations for pressure loss over air filter.

where R_f is called the *flow resistance*. d’Arcy’s law is based on empirical evidence only and it has been observed that the proportionality does not hold if the flow is not laminar. If the tube contains a sudden change in area, we have the approximate relationship

$$p(t) = \mathcal{H} \cdot Q^2(t) \cdot \text{sgn}(Q(t)) \quad (3.2)$$

for some constant \mathcal{H} . The intake and outlet of the air filter both contains sudden changes in area (i.e. (3.2) applies), furthermore the interior of the air filter is filled with a porous medium (i.e. (3.1) applies). However we do not have any possibility to measure the volumetric flow on our test bench, thus we want to describe the models as a function of mass flow, rather than volumetric flow. The relationship between these two is given by:

$$Q = \frac{\dot{m}_{\text{air}}}{\rho} = \left[\rho = \frac{p}{RT} \text{ for ideal gas} \right] = \frac{\dot{m}_{\text{air}}RT}{p}$$

Assuming that R_f in (3.1) is constant for the interior of the air filter and using the relationship between volume and mass flow given above, the pressure loss could be described as a sum of (3.1) and (3.2);

$$p_{\text{loss}} = \mathcal{H}_1 \cdot \left(\frac{\dot{m}_{\text{air}}RT_{\text{amb}}}{p_{\text{amb}}} \right) + \mathcal{H}_2 \cdot \left(\frac{\dot{m}_{\text{air}}RT_{\text{amb}}}{p_{\text{amb}}} \right)^2 \quad (3.3)$$

Note that the pressure loss due to the sudden change in area should be a function of p_{amb} at the air filter inlet and p_{comp} at the outlet, further on the pressure loss through the air filter is a function of the pressure at each cross section of it. However, p_{amb} is used in the model for simplicity.

Looking at correlations given in table 3.3 suggests that a model based on $T_{\text{amb}}\dot{m}_{\text{air}}^2$ should also be feasible;

$$p_{\text{loss}} = K T_{\text{amb}} \dot{m}_{\text{air}}^2 \quad (3.4)$$

This model is in fact the standard model used by e.g. Watson [13], but as figure 3.4 shows the model based on d’Arcy’s law gives slightly better result than the standard model.

As seen from (3.3) and (3.4), the models for the pressure loss includes both the ambient temperature and pressure, two parameters that are of limited control in the laboratory. The ambient pressure is approximately constant around 1.0 atm, while the temperature fluctuates between 293 K and 325 K, depending on e.g.

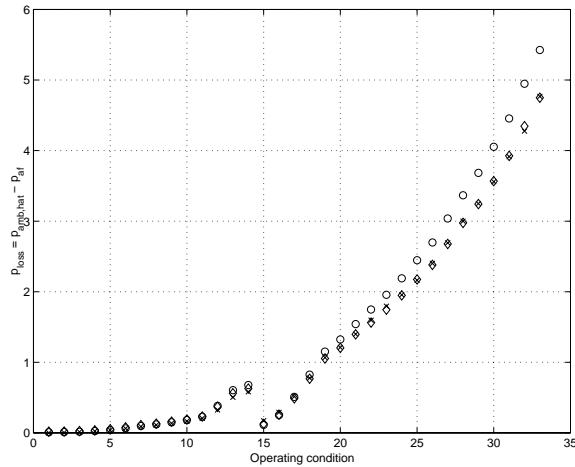


Figure 3.4 Model for pressure loss over air filter with 'x': validation points, 'o': model (3.3), 'o' model (3.4). The first 14 operating conditions are for one constant engine speed, with increasing throttle angle, and the rest are for another with increasing throttle angle.

operating condition. This means that there is no possibility to make appropriate tests for how ambient pressure and temperature affect pressure loss, thus models which are functions of mass flow only would give (almost) equally as good results as those that also includes the temperature and the pressure, but would of course be less general. At e.g. Nordic conditions the ambient temperature may, as the reader might be well aware of, go far below these limits, just as the ambient pressure would do at high altitude.

3.1.3 Air Filter Summary

$$p_{af,loss} = K T_{amb} \dot{m}_{air}^2$$

$$p_{af,loss} = \mathcal{H}_2 \cdot \left(\frac{\dot{m}_{air} R T_{amb}}{p_{amb}} \right)^2 + \mathcal{H}_1 \cdot \left(\frac{\dot{m}_{air} R T_{amb}}{p_{amb}} \right)$$

3.2 Intercooler

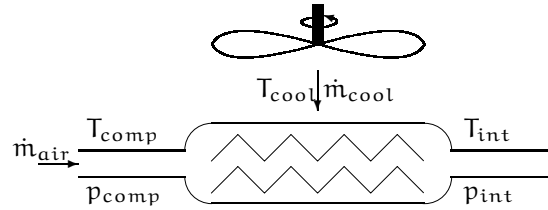


Figure 3.5 Sketch of the intercooler.

As will be explained in chapter 4, the main purpose of turbo charging an engine is to provide larger power output without increasing the size of the engine. This is done by compressing the intake air, thus increasing its density, making it possible to inject and burn more fuel in the cylinder. However, the first law of thermodynamics states that it is impossible, unless the compressor is cooled, to compress the air without raising its temperature.

By using a heat exchanger called intercooler to cool the charge air back to near ambient temperature, two desirable effects are obtained. The first is that lowering the inlet air temperature makes the temperature lower in the entire engine working process and thus providing a margin of safety to an undesired phenomenon called knock. Knock is not treated further in this report, but it is worth mentioning that it occurs when the fuel is self ignited and that it can be prevented if the temperature is kept low. Consider for example [13] for a more thorough explanation of knock. The second advantage becomes obvious when studying the equation of state for an ideal gas, $\rho = \frac{p}{RT}$. From this it is seen that the temperature rise partially offsets the benefit in density of increasing the pressure.

The ability for the intercooler to lower the temperature is characterized by a measure of efficiency, ε , which may be defined as:

$$\varepsilon = \frac{\text{actual heat transfer}}{\text{maximum possible heat transfer}}$$

The maximum value of heat transfer could be attained if one of the fluids were to undergo a temperature change equal to the maximum temperature difference in the heat exchanger, which is the difference in entering temperatures for the hot and the cool fluid. If both the fluids present in the exchanger are air, conservation of energy requires that the fluid that undergoes this maximum temperature change is the one with the minimum value of the air mass flow rate. For all practical purposes of an intercooler, this is \dot{m}_{air} , i.e. the compressor outlet flow. Then the

expression for ε becomes:

$$\varepsilon = \frac{T_{\text{comp}} - T_{\text{int}}}{T_{\text{comp}} - T_{\text{cool}}}$$

hence T_{int} , which is the parameter of interest, can be expressed as:

$$T_{\text{int}} = T_{\text{comp}} - \varepsilon (T_{\text{comp}} - T_{\text{cool}}) \quad (3.5)$$

where T_{comp} is the compressor outlet air temperature and T_{cool} is the temperature of the cooling medium, in this case the ambient air temperature.

To achieve efficient cooling of the charge air, the tubes in the intercooler need to be rather thin in order to expose as much as possible of the air to the cooling medium. The result is that some of the gain in intake air density is lost. Therefore, besides models for the outlet air temperature, also a model for the pressure loss need to be developed. This is done in the following sections.

3.2.1 Intercooler Measurement Procedures

The following experiment was performed on the intercooler:

- \dot{m}_{air} , T_{comp} , T_{int} , T_{cool} , p_{comp} and p_{int} were measured for different engine speeds and throttle plate positions
- N ranges from 1300 rpm to 4800 rpm with steps of 500 rpm.
- α is varied in the entire engine working area.
- The parameters of interest were measured during 3 seconds and then averaged after waiting 1 minute between each change in operating conditions for stabilization of pressures and temperatures. Between each series of engine speeds, that is when changing from one engine speed to a higher and decreasing the throttle angle at the same time, the engine is run several minutes to secure stationary conditions.
- The measurements were repeated for three different speeds of the intercooler fan: 30%, 60% and 90% of maximum speed.

The cooling air mass flow, \dot{m}_{cool} , could not be measured in the laboratory, but by estimating the air speed for maximum fan speed and making the assumption that the air speed is proportional to the fan speed, a value of \dot{m}_{cool} is obtained from the relation:

$$\dot{m}_{\text{cool}} = \rho_a A v_{\text{cool}}$$

where ρ_a is the ambient air density, A the intercooler front area and v_{cool} is the air speed i.e. the velocity of the car. To get an idea of the order of \dot{m}_{cool} , assume $A = 0.25 \text{ m}^2$, $v_{\text{cool}} = 70 \text{ km/h} = 25 \text{ m/s}$ and $\rho_a = 1.293 \text{ kg/m}^3$ which gives $\dot{m}_{\text{cool}} \approx 30 \times 10^3 \text{ kg/h}$.

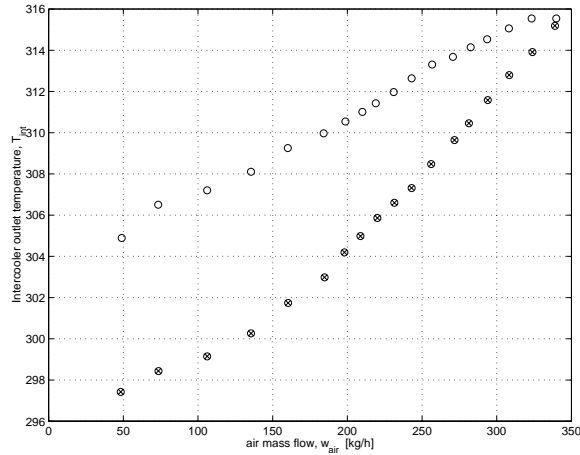


Figure 3.6 Intercooler outlet air temperature dependence on air mass flow. \otimes marks increasing throttle angle. \times decreasing. Differences between measurements is due to not waiting enough after change in throttle plate position before making measurements. That is we do not have stationary conditions.

A problem when measuring the intercooler properties is that, when changing the throttle plate position and thus changing the operating conditions of the engine, it takes quite long time for the temperatures to reach stationary level. To get a hint of what can be a reasonable time period to wait between measurements, experiments were performed measuring the intercooler outlet air temperature, T_{int} , while the throttle plate opening area was first increased stepwise and then returned to its initial position. Increasing the opening area increases the air mass flow into the engine, causing it to reach a higher operating condition with an increase in temperature as a consequence.

In figure 3.6, intercooler outlet temperature is plotted for increasing air mass flows in the same diagram as the one for decreasing mass flows. For both series the time between each sample is the same but, as the figure shows, the temperatures for a certain air mass flow does not correlate between the two different series, hence stationary conditions is not reached for at least one of the series.

Further investigations shows that it takes less than one minute to reach stationary conditions when increasing the throttle angle and about a ten times longer interval is needed during decrease. As it would take too much time to wait about ten minutes between every change in operating condition, measurements are done for increasing throttle positions only.

3.2.2 Temperature Models

Assuming that \dot{m}_{air} is less than \dot{m}_{cool} , as mentioned earlier, the intercooler outlet temperature is given by equation (3.5). From this expression it is seen that in order to predict the intercooler outlet temperature, one needs a model for the intercooler efficiency, ε . Figure 3.7 illustrates the intercooler architecture used in the

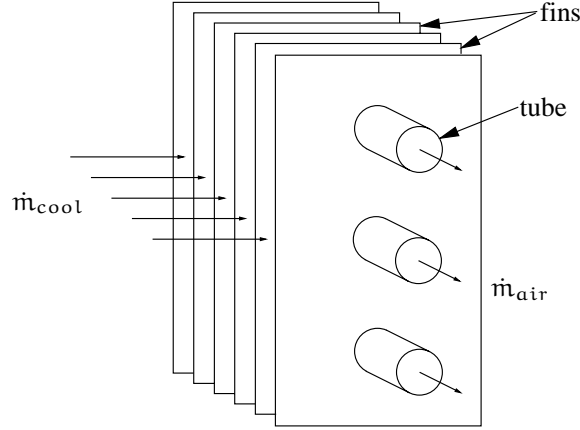


Figure 3.7 Cross flow, both fluids unmixed intercooler

experiments in this section. The air flowing across the finned tube as well as the air flowing in the tubes is said to be unmixed since it is confined in separate channels between the fins and tubular channels respectively, so that it can not mix with itself during the heat transfer process. For this reason, an intercooler of this type is referred to as a *Cross flow intercooler, both fluids unmixed*.

Expressions for numerous intercooler architectures are listed in [5] and for an architecture as described above, it is stated as:

$$\varepsilon = 1 - e^{-\frac{e^{-N^{0.78}} C - 1}{N^{0.22} C}} \quad (3.6)$$

where

$$N = \frac{UA}{C_{\min}}, \quad C = \frac{C_{\min}}{C_{\max}}$$

and

$$C_{\min} = (\dot{m}c_p)_{\min}, \quad C_{\max} = (\dot{m}c_p)_{\max}, \quad c_p = c_{p,\text{air}}$$

If \dot{m}_{air} is recognized as the minimum fluid, these expressions can be rewritten:

$$\dot{m}_{\text{air}} < \dot{m}_{\text{cool}} \Rightarrow C_{\min} = \dot{m}_{\text{air}}c_{p,\text{air}}, \quad C_{\max} = \dot{m}_{\text{cool}}c_{p,\text{air}}$$

This gives:

$$N = \frac{UA}{c_{p,air}\dot{m}_{air}}, \quad C = \frac{\dot{m}_{air}}{\dot{m}_{cool}}$$

where A is a constant denoting some effective surface for the heat transfer. U is the overall heat transfer coefficient, describing the combined heat transfer by convection on the inner tube surface, conduction inside the tube material and again convection on the outer tube surface. See e.g. [5] for further explanations of the heat transfer processes involved.

If the inside and outside area of the tubes are considered approximately equal and the amount of heat transfer from conduction is neglected, the overall heat transfer coefficient U can be written as:

$$U = \frac{1}{\frac{1}{h_i} + \frac{1}{h_o}}$$

The main subject is to model the convection heat transfer coefficients, h_i and h_o , for the inside and the outside of the tubes respectively. For turbulent fluid flow through smooth tubes the following empirical relation between the Nusselts² (Nu), Prandtl³ (Pr) and Reynolds⁴ (Re) numbers is recommended in [5] (In the below expressions K_1, K_2, \dots denotes constants):

$$Nu = K_1 Re^{0.8} Pr^{0.3} \quad (3.7)$$

The Nu , Pr and Re numbers are groupings of different properties for the fluids involved in the heat transfer and for simplicity, in this text the properties that can be assumed constant are lumped together and are not explained further. For our purposes, these numbers can be written in the following, simplified form:

$$Nu = K_2 h, \quad Re = K_3 \frac{\dot{m}}{\mu}, \quad Pr = K_4 \mu$$

where h is the convection heat transfer coefficient, μ is the dynamic viscosity and \dot{m} is the mass flow rate of the fluids involved. Inserting the above in equation (3.7) gives an expression for h :

$$h = K_5 \dot{m}^{0.8} \mu^{-0.5}$$

μ is a strongly temperature dependent parameter and is modeled by simply fitting an exponential function to the values of the dynamic viscosity tabulated in [4]. If

²Named in honor of Wilhelm Nusselt (1882-1957) who was nominated Professor of theoretical and Mechanical Engineering at the Technische Hochschule, Karlsruhe in 1920. Between 1925 and 1952 he taught at the Technische Hochschule, München. He published his fundamental work "The Fundamental Laws of Heat Transfer" in 1915.

³Born in Germany, Ludwig Prandtl (1875-1953) taught at Hannover Engineering College and then Göttingen University. He is called the creator of modern fluid mechanics.

⁴Osborne Reynolds (1842-1912), English physicist and professor who presented this in a publication of his experimental work in 1882.

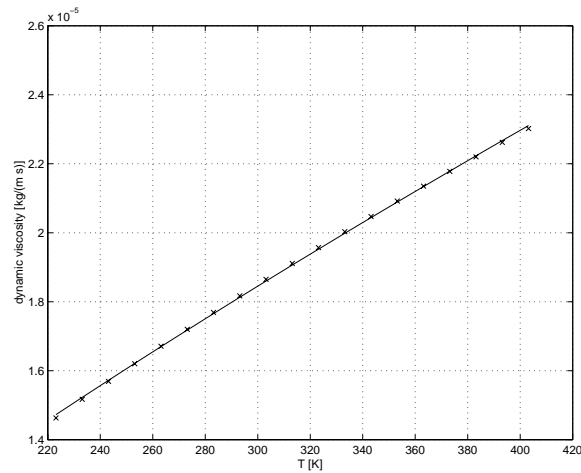


Figure 3.8 x: Tabulated values for the dynamic viscosity of dry air at atmospheric pressure plotted versus temperature. The solid line is the fitted model.

the model is calculated for tabulated values in the temperature interval ranging from 220K to 400K, which should cover the interesting temperatures by margin, the following expression for μ can be used:

$$\mu = 2.3937 \cdot 10^{-7} T^{0.7617} \quad (3.8)$$

Figure 3.8 shows the tabulated values and the fitted curve respectively, plotted versus temperature.

To determine the temperatures at which μ_i and μ_o should be evaluated, some further simplifications has to be made in order to get a reasonable complexity of the model. These includes:

- The temperature of the outside of the intercooler tubes is constant and equal to the cooling air temperature, T_{cool} , so that

$$T \approx T_{cool}$$

for the outside heat transfer process.

- The mean temperature of the air inside the intercooler tubes is taken as the average of the entering air temperature, T_{comp} , and T_{cool} . That is:

$$T \approx \frac{T_{comp} + T_{cool}}{2}$$

for the heat transfer inside the tubes.

A more accurate calculation of the mean temperature inside the tubes should use the real exit temperature T_{int} instead of T_{cool} , but this is certainly increasing the difficulty calculating T_{int} from equation (3.5). In this case the equation takes the form:

$$\begin{aligned} T_{\text{int}} &= T_{\text{comp}} - \epsilon (T_{\text{comp}} - T_{\text{cool}}) = \\ &= T_{\text{comp}} - \left(1 - e^{-\frac{e^{\frac{f_1(T_{\text{int}})-1}{f_2(T_{\text{int}})}}}{N}} \right) (T_{\text{comp}} - T_{\text{cool}}) \end{aligned}$$

and this equation can not be solved analytically for T_{int} , instead some numerical method has to be used. However, the above approximations of T results in the following expressions for the inside and outside convection heat transfer coefficients:

$$\begin{aligned} h_i &= K_5 \dot{m}_{\text{air}}^{0.8} \mu_i^{-0.5}, \quad \mu_i = 2.3937 \cdot 10^{-7} \left(\frac{T_{\text{comp}} + T_{\text{cool}}}{2} \right)^{0.7617} \\ h_o &= K_6 \dot{m}_{\text{cool}}^{0.8} \mu_o^{-0.5}, \quad \mu_o = 2.3937 \cdot 10^{-7} T_{\text{cool}}^{0.7617} \end{aligned}$$

From the $30 \cdot 10^3$ kg/h estimation of \dot{m}_{cool} in section (3.2.1) and a typical value of \dot{m}_{air} of approximately 300 kg/h, it seems reasonable to neglect the term $\frac{1}{h_o}$ in U , in comparison with $\frac{1}{h_i}$. Thus the overall heat transfer coefficient is simplified to $U = h_i$. To summarize the above discussion, the model for ϵ to use in equation (3.5) becomes:

$$\begin{aligned} \epsilon &= 1 - e^{-\frac{e^{-N^{0.78} C - 1}}{N - 0.222 C}} \\ N &= \frac{K}{c_{p,\text{air}}} \dot{m}_{\text{air}}^{-0.2} \mu_i^{-0.5} \\ \mu_i &= 2.3937 \cdot 10^{-7} \left(\frac{T_{\text{comp}} + T_{\text{cool}}}{2} \right)^{0.7617} \\ C &= \frac{\dot{m}_{\text{air}}}{\dot{m}_{\text{cool}}} \end{aligned}$$

The unknown constant K is determined from a least squares fit to measured data and as can be seen, the model is now expressed in variables that can easily be measured or estimated. Figure 3.9 shows the modeled and real values for ϵ and T_{int} respectively and it shows that for low values of \dot{m}_{air} , the modeled efficiency deviates quite a lot from the measured. Several reasons are conceivable; the assumptions made when estimating \dot{m}_{cool} might be erroneous, the conditions for the actual fluid flow in the tubes does perhaps not quite fulfill the requirements for equation (3.7) to express the correct relationship between the Nu , Re and Pr

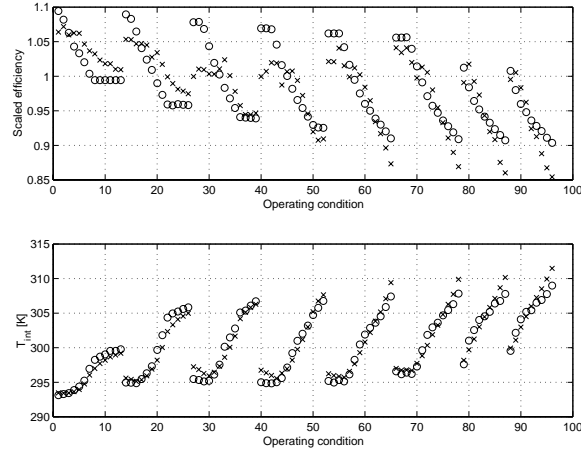


Figure 3.9 *x*: Measured values, diamond: Predicted. The figure shows measured and predicted values for ε and T_{int} respectively for the case of 60% fan speed. Maximum error: 2.5K.

numbers etc. Fortunately, since the error for ε is largest for low values of \dot{m}_{air} , where T_{comp} also is rather low, the error when calculating T_{int} with (3.5) is reasonably small and as can be seen in the bottom plot of figure 3.9, the agreement between model and reality is fairly good.

Another approach for modeling ε would be to use the above calculations only as an indicator of which parameters that affect the efficiency and use them as regressors in a linear regression model. Choosing the mean tube temperature and air mass flow together with the ratio of the air mass flow and the cooling air mass flow, the following model for ε may be stated;

$$\varepsilon = a_0 + a_1 \left(\frac{T_{comp} + T_{cool}}{2} \right) + a_2 \dot{m}_{air} + a_3 \frac{\dot{m}_{air}}{\dot{m}_{cool}} \quad (3.9)$$

The result is displayed in figure 3.10 and it shows that this model has somewhat better correlation with T_{int} than the previous, but might be less general.

3.2.3 Pressure Models

The intercooler may be described as a thin and long tube, with some direction changes, cooled by the surrounding air. The pressure losses stem from friction against the walls and the direction changes. Nakayama [8] states that both losses are proportional to the squared mass flow. Thus both (3.3) and (3.4) should give a good description of the pressure loss over the intercooler. With the assumption

that the pressure loss due to change of direction depends only on the squared mass flow (3.3) could be simplified;

$$p_{\text{loss}} = \mathcal{H} \cdot \left(\frac{\dot{m}RT_{\text{comp}}}{p_{\text{comp}}} \right)^2 \quad (3.10)$$

As figure 3.11 shows, all models give very similar results, and the simplified or the standard model are preferable as they have less predictors than (3.3).

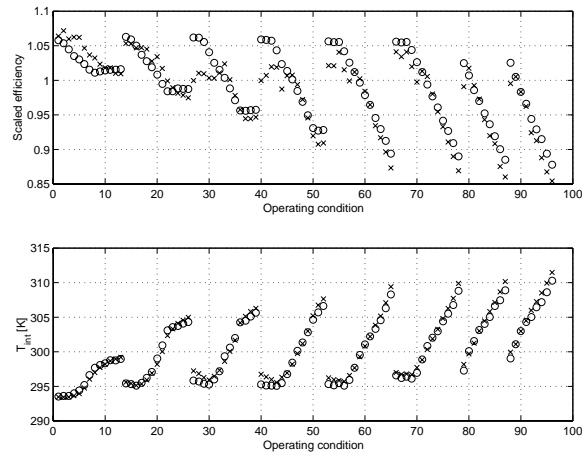


Figure 3.10 *x*: Measured values, *o*: Predicted. The figure shows measured and predicted values for ϵ and T_{int} respectively for the case of 60% fan speed. Maximum error: 1.5K.

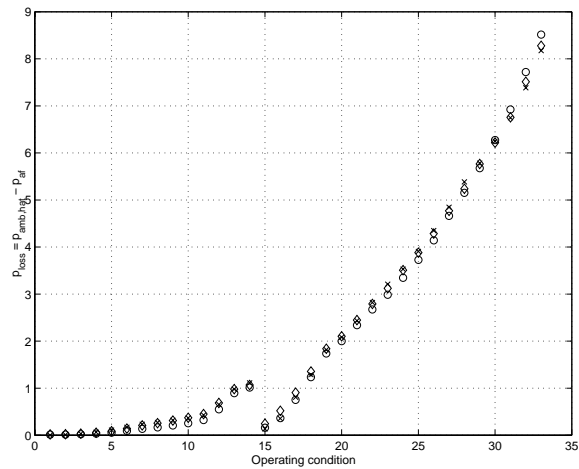


Figure 3.11 Model for pressure loss over intercooler with 'x': validation points, 'o': model (3.3), 'o': model (3.10) '-'. Note that (3.3) and (3.4) coincides almost exactly, therefor (3.4) is not plotted in this figure. The first 14 operating conditions are for one constant engine speed, with increasing throttle angle, and the rest for another with increasing throttle angle.

3.2.4 Intercooler Summary

$$T_{\text{int}} = T_{\text{comp}} - \varepsilon (T_{\text{comp}} - T_{\text{cool}})$$

ε - model 1:

$$\varepsilon = 1 - e^{-\frac{e^{-N^{0.78} C - 1}}{N^{-0.22} C}}$$

$$N = \frac{K}{c_{p,\text{air}}} \dot{m}_{\text{air}}^{-0.2} \mu_i^{-0.5}$$

$$\mu_i = 2.3937 \cdot 10^{-7} \left(\frac{T_{\text{comp}} + T_{\text{cool}}}{2} \right)^{0.7617}$$

$$C = \frac{\dot{m}_{\text{air}}}{\dot{m}_{\text{cool}}}$$

ε - model 2:

$$\varepsilon = a_0 + \frac{a_1}{1000} \left(\frac{T_{\text{comp}} + T_{\text{cool}}}{2} \right) + \frac{a_2}{1000} \dot{m}_{\text{air}} + a_3 \frac{\dot{m}_{\text{air}}}{\dot{m}_{\text{cool}}}$$

$$p_{\text{int,loss}} = K T_{\text{comp}} \dot{m}_{\text{air}}^2$$

$$p_{\text{int,loss}} = \mathcal{H} \cdot \left(\frac{\dot{m}_{\text{air}} R T_{\text{comp}}}{p_{\text{comp}}} \right)^2$$

3.3 Throttle

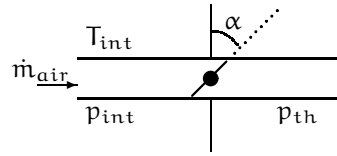


Figure 3.12 Sketch of throttle.

The throttle is used to control the air mass flow in the intake system. The throttle motion is governed by an electrical servo, which can be modeled using standard DC motor models and a friction model (see [19]). The main interest though, is to model the air mass flow through the throttle. This has been done by e.g. Heywood [12] and Müller [15].

3.3.1 Throttle Measurement Procedures

The following experiment was performed on the throttle:

- \dot{m}_{air} , T_{int} , p_{int} and p_{th} were measured for different engine speeds and throttle plate positions.
- N ranges from 1500 rpm to 4500 rpm with steps of 500 rpm.
- α is varied in the entire engine working area.
- The parameters of interest were measured during 3 seconds and then averaged after waiting 10 seconds between each change in operating condition for stabilization of pressure and temperatures.

3.3.2 Air Mass Flow Model

A standard approach when modeling the throttle plate air mass flow, \dot{m}_{air} , is to consider the air mass flow through a venturi, which is given by

$$\dot{m}_{air}(\alpha, p_{in}, p_{out}, T_{in}) = \frac{p_{in}}{\sqrt{RT_{in}}} Q(\alpha) \Psi(p_r)$$

where Q is a function that depends on the opening area, A_{th} , and a discharge coefficient, C_d , that depends on the shape of the flow area;

$$Q_{th} = A_{th} C_d$$

and $\Psi(p_r)$ is a nonlinear function of the pressure ratio, $p_r = \frac{p_{out}}{p_{in}}$, and is given by

$$\Psi(p_r) = \begin{cases} \sqrt{\frac{2\gamma}{\gamma-1} \left(p_r^{\frac{2}{\gamma}} - p_r^{\frac{\gamma+1}{\gamma}} \right)} & \text{for } p_r > \left(\frac{2}{\gamma+1} \right)^{\frac{\gamma}{\gamma-1}} \\ \sqrt{\frac{2\gamma}{\gamma-1} \left(\left(\frac{2}{\gamma+1} \right)^{\frac{2}{\gamma-1}} - \left(\frac{2}{\gamma+1} \right)^{\frac{\gamma+1}{\gamma-1}} \right)} & \text{else} \end{cases}$$

This gives the following model for the throttle:

$$\dot{m}_{air}(\alpha, p_{int}, p_{th}, T_{int}) = \frac{p_{int}}{\sqrt{RT_{int}}} Q_{th}(\alpha) \Psi(p_{r,th}) \quad (3.11)$$

where

$$p_{r,th} = \frac{p_{th}}{p_{int}}$$

Nyberg [20] suggests the following simple physical model for the opening area:

$$A_{th} = A_1(1 - \cos(\alpha_0\alpha + \alpha_1)) + A_0$$

where A_1 is the area that is covered by the throttle plate when the throttle is closed and A_0 is the *leak area* present even though the throttle is closed. The parameters α_0 and α_1 are compensation for that the actual measured throttle angle may be scaled and biased because of production tolerances. The discharge coefficient, C_d , is assumed to be constant, thus

$$Q_{th} = Q_1(1 - \cos(\alpha_0\alpha + \alpha_1)) + Q_0 \quad (3.12)$$

More complex, and physical correct, models are presented by e.g. Heywood, but they fail to give a better fit to sampled data. A couple of other models (found by looking at correlations) were also tested;

$$Q_{th}(\alpha) = a_2\alpha^2 + a_1\alpha + a_0 \quad (3.13)$$

$$Q_{th}(\alpha) = a_2\cos^2\alpha + a_1\cos\alpha + a_0 \quad (3.14)$$

These models lack the physical background of (3.12) but nevertheless shows almost as good fit to available data. The average error is below 2% for all of them, but as (3.12) could be expected to have better extrapolating capabilities, due to its physical background, it is preferable to select this model over the other two. A validation of this model is shown in figure 3.13.

Remarks on turbulence It is clear from geometrical considerations and flow visualization studies that the flow around a typical throttle can not be isentropic, see figure 3.14. If this is considered, a more accurate physical model may be developed. This is not done in this thesis (refer to [17] for a brief study), but the effects

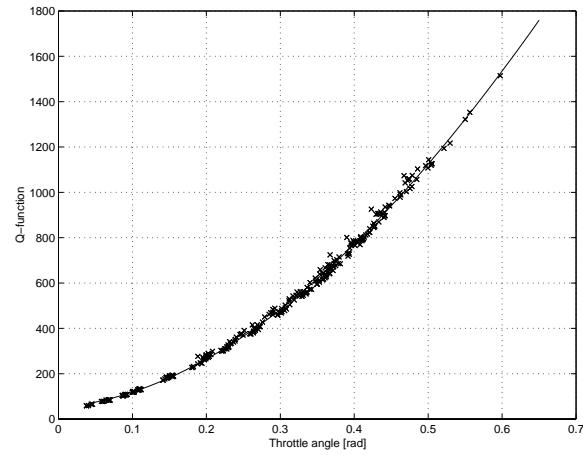


Figure 3.13 Validation of (3.12), with Q plotted versus throttle angle. The solid line marks the model and 'x' marks validation points.

should not be too significant. Furthermore, the flow characteristics depend on how the manufacturer has chosen to construct the throttle plate.

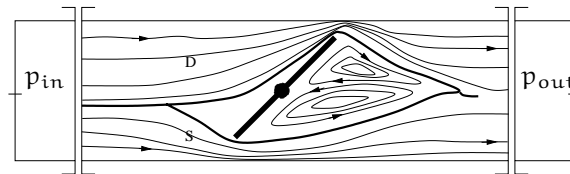


Figure 3.14 Approximate air mass flow distribution through throttle. D and S denote Dominant and Subordinate flow paths.

3.3.3 Throttle Summary

$$\begin{aligned}\dot{m}_{\text{air}}(\alpha, p_{\text{int}}, p_{\text{th}}, T_{\text{int}}) &= \frac{p_{\text{int}}}{\sqrt{RT_{\text{int}}}} Q_{\text{th}}(\alpha) \Psi(p_{r,\text{th}}) \\ Q_{\text{th}} &= Q_1(1 - \cos(a_0\alpha + a_1)) + Q_0\end{aligned}$$

3.4 Intake System Dynamics

3.4.1 Pressure Dynamics

As can be seen in figure 2.1 the compressor outlet air has to pass through a tube to the intercooler, through the intercooler and another tube, past the throttle to the intake manifold before it enters the engine. The total volume of the intake system is of the order 10–15 litres and therefore, for a sudden increase in the inlet air mass flow it takes some time for the flowing air to fill the volume and to build up the pressure in the intake system. An example is shown in figure 3.15, where the air mass flow and the intake manifold pressure were measured for a series of sudden changes of the throttle plate angle.

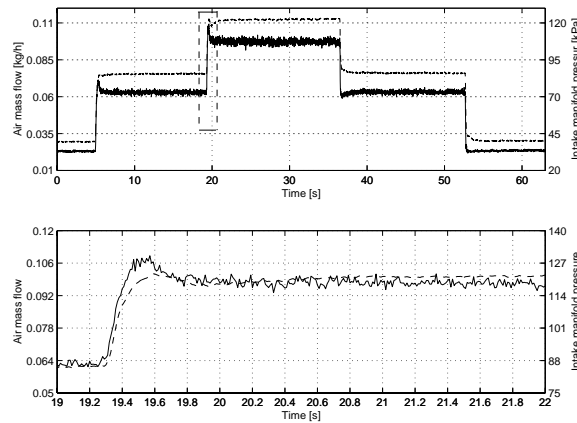


Figure 3.15 The top of the figure shows manifold pressure and air mass flow into the manifold for a series of sudden changes in throttle angle. The box shows the zoom area for the bottom plot.

In this thesis a model for the pressure build-up in the intake manifold is developed using a balance equation expressing the conservation of mass in the manifold:

$$\text{Mass Flow entering} - \text{Mass Flow leaving} = \text{Stored mass per unit of time} \quad (3.15)$$

where the air mass flow entering and leaving would be the flow past the throttle and the flow entering the engine respectively. A more complete model, better suited for dynamic operation should include a similar model for the volume consisting of the tubings and the intercooler. In this case the entering and leaving flow is that from the compressor and past the throttle respectively. Looking at figure 2.4 it is seen that this would require changing the current model structure for the compressor to express the air mass flow through the compressor as a function of the shaft speed and the ratio of the outlet and the inlet pressure, that is:

$\dot{m}_{air} = f(N_t, p_r)$ rather than the existing: $p_r = f(N_t, \dot{m}_{air})$. This also affect other models such as for the air filter and the turbo shaft speed and is not done, but is left to future projects.

For the intake manifold, equation (3.15) becomes:

$$\frac{d}{dt} m_{air,man} = \dot{m}_{air} - \dot{m}_{air,c} \quad (3.16)$$

where $m_{air,man}$ is the air mass in the manifold, \dot{m}_{air} is the air mass flow past the throttle as stated in equation (3.11) and $\dot{m}_{air,c}$, the air mass flow into the cylinders is calculated below. Note that in this section SI units are used instead of those given in the nomenclature.

The volumetric efficiency, η_{vol} , is a measure of the effectiveness of the engine to induct fresh air and is defined as the ratio of the actual volume flow rate of air entering the cylinders, $\frac{\dot{m}_{air,c}}{\rho_{air,man}}$, and the rate at which volume is displaced by the piston, $\frac{V_d N}{2 \times 60}$. The factor 2 in the denominator arise from the fact that the engine inducts fresh air in each cylinder every second revolution only. Using the above, the expression for the volumetric efficiency becomes:

$$\eta_{vol} = 120 \frac{\dot{m}_{air,c}}{\rho_{air,man} V_d N} = \left[\rho_{air,man} = \frac{p_{man}}{RT_{man}} \right] = 120 \frac{\dot{m}_{air,c} RT_{man}}{p_{man} V_d N} \quad (3.17)$$

In order to determine η_{vol} , experiments were performed running the engine at a large number of different speeds and throttle positions. When T_{man} , which is the slowest parameter, has reached a stationary value, p_{man} , T_{man} and \dot{m}_{air} were measured. Note that for stationary conditions, no mass is stored in the manifold so that the air mass flow into the cylinder equals that past the throttle and thus $\dot{m}_{air,c} = \dot{m}_{air}$. Using equation (3.17) to calculate η_{vol} for each set of measured values and plot it versus N and p_{man} gives a η_{vol} map shown in figure 3.16. When the volumetric efficiency is mapped, $\dot{m}_{air,c}$ can be calculated from (3.17).

$$\dot{m}_{air,c} = \frac{\eta_{vol} V_d N}{120 R T_{man}} p_{man} \quad (3.18)$$

Using the ideal gas equation of state for the manifold, $m_{air,man}$ in (3.16) can be expressed in terms of p_{man} in the following way:

$$m_{air,man} = \frac{V_{man}}{R T_{man}} p_{man} \quad (3.19)$$

If equation (3.19) is differentiated, the left hand side in (3.16) can be determined.

$$\frac{d}{dt} m_{air,man} = \frac{V_{man}}{R} \frac{d}{dt} \left(\frac{p_{man}}{T_{man}} \right) = \frac{V_{man}}{R T_{man}} \left[\frac{d}{dt} p_{man} - \frac{p_{man}}{T_{man}} \frac{d}{dt} T_{man} \right] \quad (3.20)$$

The variations in T_{man} is very slow in comparison to changes in p_{man} and therefore the last term in (3.20) is neglected, that is:

$$\frac{d}{dt} m_{air,man} = \frac{V_{man}}{R T_{man}} \frac{d}{dt} p_{man} \quad (3.21)$$

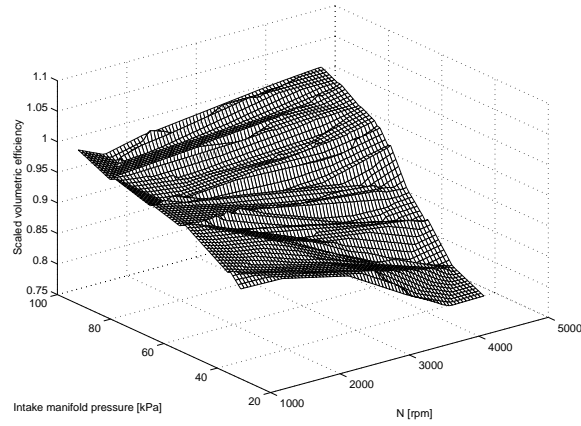


Figure 3.16 Volumetric efficiency map.

Finally, inserting equations (3.18) and (3.21) in (3.16) results in the following dynamic equation for the manifold pressure:

$$\frac{d}{dt}p_{\text{man}} + \frac{\eta_{\text{vol}}V_dN}{120V_{\text{man}}}p_{\text{man}} = \frac{RT_{\text{man}}}{V_{\text{man}}}\dot{m}_{\text{air}} \quad (3.22)$$

Figure 3.17 shows a validation of this model for a sudden change in throttle angle. The air mass flow entering the intake manifold, \dot{m}_{air} , could not be measured during the transient, but is calculated from the model in section 3.3.

3.4.2 Temperature Dynamics

Another dynamic aspect that should be considered is that for the intercooler outlet temperature. However faster temperature sensors are needed to perform appropriate experiments, therefore temperature dynamics are not considered further in this thesis, but should be studied in future projects.

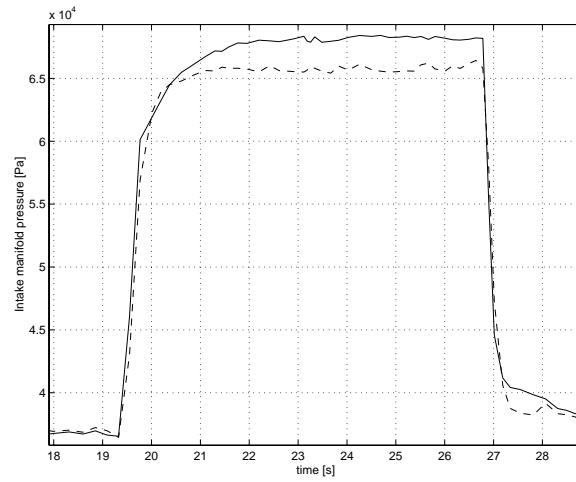


Figure 3.17 Validation of the intake manifold pressure model for $N = 1500$ rpm with a step change in throttle angle. Solid line: measured pressure. Dashed: predicted.

3.4.3 Intake Manifold Summary

$$\frac{d}{dt}p_{\text{man}} + \frac{\eta_{\text{vol}}V_dN}{120V_{\text{man}}}p_{\text{man}} = \frac{RT_{\text{man}}}{V_{\text{man}}}\dot{m}_{\text{air}}$$

Remark: SI units are used in this equation.

Chapter 4

Turbo

The maximum power a given engine can deliver is limited by the amount of fuel that can be burned efficiently inside the engine cylinder. This is limited by the amount of air that is inducted into each cylinder each cycle. If the inducted air is compressed to a higher density than ambient, prior to entry into the cylinder, the maximum power an engine of fixed dimensions can deliver will be increased. This is the primary purpose of the turbo charger.

The most difficult part when modeling turbo engines is the modeling of the turbo charger dynamics. Several models are presented by e.g. Müller [15], Moraal [14] and Watson & Janota [13]. Most existing models are performance maps, consisting of a collection of known operating conditions. Interpolation is used to calculate intermediate operating conditions. Due to the following problems these models are not satisfactory:

- Accuracy is highly dependent on the amount of data available.
- Questionable extrapolating capability.
- Model implementation is not exact.
- Table look-up induces numerical noise (discontinuities).
- No basis for extrapolation in surge region (see figure 4.3).

By developing models based on physical relationships it is likely, but not certain, that extrapolating capabilities will improve. However no investigation is performed with respect to extrapolation.

4.1 Compressor Nomenclature

The following nomenclature and units are used in chapter 4.2 to describe internal signals velocity triangles for the compressor.

<i>Symbol</i>	Quantity (explanation)	unit
A_1	inducer inlet cross sectional area	m^2
C_1	absolute air velocity entering the inducer	m/s
C_2	absolute air velocity leaving impeller tip	m/s
D_1	representative diameter of inducer inlet area	m
D_2	impeller tip diameter	m
U_1	inducer blade representative velocity	m/s
$U_c (U_2)$	impeller tip speed	m/s
W_1	air velocity relative to the inducer blade	m/s
W_2	air velocity relative to the rotor blades	m/s
$W_{\theta 1}$	desctructed component of W_1	m/s
β	backswEEP angle	rad
β_2	relative flow angle at impeller tip	rad
β_{2b}	impeller backswEEP angle	rad
β_{opt}	optimal relative flow angle, resulting in zero incidence loss	rad
ρ_1	compressor inlet static density	kg/m^3

Subscripts

r	radial component
θ	tangential component

4.2 Compressor

To counteract the density loss due to the increase in temperature it is desirable to achieve a compression process that approaches the isentropic, since this process yields the least temperature rise. It is true that the compressed air is cooled in the intercooler, but as could be seen in section 3.2, lower intercooler inlet temperature results in overall lower temperature in the intake system and thus a higher air density. Depending on the structure of the models of the other engine subsystems, two different approaches for the compressor model are feasible. That is to either model the flow through the compressor as a function of pressure ratio and turbo shaft speed, or the pressure ratio as a function of compressor flow and turbo shaft speed. As the compressor flow is given by the air mass flow model for the throttle in the stationary case, the latter version is chosen.

4.2.1 Compressor Geometry

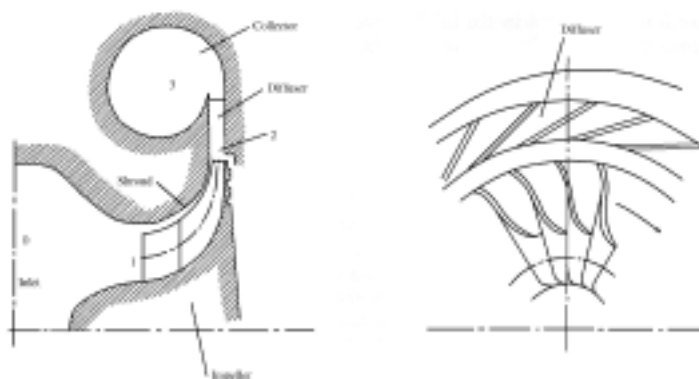


Figure 4.1 Components of centrifugal compressor

In this section the compressor geometry is presented, to set each part of the compressor into context this is done by giving an explanation for what happens at respective part. The radial flow, or centrifugal, compressor is made up from four basic components or sections

0. Stationary inlet casing.
1. Rotating impeller.
2. Stationary diffuser of the vaneless type.
3. Collector or volute.

These components are denoted by respective number in figure 4.2.1. In some compressors guide vanes have been fitted in the inlet casing, principally to enable some control to be exercised on the flow characteristics. However this is not the case for the compressor studied here. The studied compressor has an axial inlet flow into the inlet casing, which simply directs the air flow into the impeller eye, or inducer. Since the velocity of the air must increase as it approaches the eye, its static pressure will decrease accordingly. In the impeller the blades impart a swirling motion on the air, which leaves the impeller tip outer diameter, D_2 , at high velocity. Work transfer takes place in the impeller and the static pressure of the air increases from the inducer to the impeller tip due to the centripetal acceleration. The purpose of the diffuser is to convert the high velocity of the air leaving the impeller into pressure by slowing it down carefully to an acceptable level, that is to diffuse. The collector or volute collects the gases from around the circumference of the diffuser and delivers it to the exit duct, which leads to the intercooler.

4.2.2 Physical Relationships for Compressor

From the first law of thermodynamics the following relationship can be established for a quasi equilibrium adiabatic process of an ideal gas with constant specific heats:

$$pv^\gamma = \text{const}$$

For such a process between states 1 and 2, the following equality may be stated:

$$p_1 v_1^\gamma = p_2 v_2^\gamma \quad (4.1)$$

Using the ideal gas equation of state $pv = RT$ in state 1 and 2 gives:

$$\frac{p_1 v_1}{T_1} = \frac{p_2 v_2}{T_2} \quad (4.2)$$

If (4.1) and (4.2) are combined, the expression for isentropic compression between states 1 and 2 is obtained:

$$\frac{p_2}{p_1} = \left(\frac{T_{2, \text{is}}}{T_1} \right)^{\frac{\gamma}{\gamma-1}} = \left(1 + \frac{\Delta T_{\text{is}}}{T_1} \right)^{\frac{\gamma}{\gamma-1}} \quad (4.3)$$

As mentioned, the above expressions is valid only if the process is isentropic, i.e. no change in entropy. This process is illustrated with the solid vertical line in the enthalpy-entropy diagram in figure 4.2. In a real process there are always losses and the compression deviates from the ideal isentropic case. The dotted line in figure 4.2 shows that change in enthalpy and thus in the temperature is larger for the real process. To account for the fact that the real process is not isentropic, the compressor isentropic efficiency, η_c , is introduced and defined as:

$$\eta_c = \frac{\text{isentropic work}}{\text{actual work}}$$

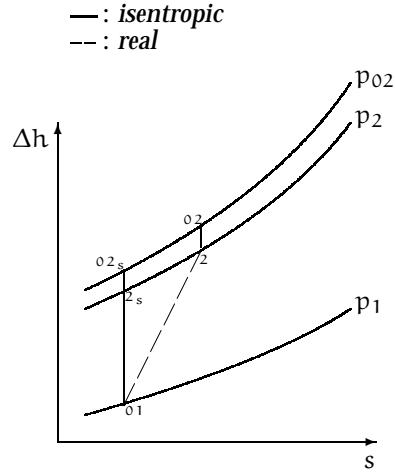


Figure 4.2 Figure illustrating the difference between an isentropic and a real compression process.

Below, two versions of this definition are stated; η_{cTT} and η_{cTS} where the subscripts TT and TS denotes *Total to Total* and *Total to Static* respectively.

$$\eta_{cTT} = \frac{h_{02s} - h_{01}}{h_{02} - h_{01}} = \frac{T_{02s} - T_{01}}{T_{02} - T_{01}}$$

$$\eta_{cTS} = \frac{h_{2s} - h_{01}}{h_{02} - h_{01}} = \frac{T_{2s} - T_{01}}{T_{02} - T_{01}} \quad (4.4)$$

The right hand equality arise from the assumption of constant specific heat c_p . The difference between the above expressions is the pressure of the compressed air in the final state. The outlet pressure has both a static and a dynamic part, where the latter originate from the kinetic energy in the air flow. This is also illustrated in figure 4.2, where index 2 refers to the static part and 02 to the sum of the static and the dynamic part, called the total or stagnation pressure. If it is assumed that this kinetic energy can be utilized by the engine, which can be realistic for some compressor types, η_{cTT} can be used. However, due to the relatively large volume of the intake manifold, the speed of the compressed air is low and therefore one assumes that only the static part of the pressure is utilized. Therefore η_{cTS} is a more correct measure of the efficiency in our case. No matter which of the expressions for the efficiency is chosen, it relates the isentropic and the actual temperature change as:

$$\Delta T_{is} = \eta_c \Delta T \quad (4.5)$$

so that the relation between pressure ratio and actual temperature change over the compressor becomes

$$\frac{p_2}{p_1} = \left(1 + \frac{\eta_c \Delta T}{T_1}\right)^{\frac{\gamma}{\gamma-1}} \quad (4.6)$$

or similarly, since $\Delta T = \frac{\Delta h}{c_p}$:

$$\frac{p_2}{p_1} = \left(1 + \frac{\eta_c \Delta h}{T_1 c_p}\right)^{\frac{\gamma}{\gamma-1}} \quad (4.7)$$

If the compressor is considered to be a steady-flow, open system, it can be analyzed as in appendix B.2. Neglecting heat transfer with the surroundings, change in potential energy and using the concept of total enthalpy, the expression for the first law of thermodynamics is reduced to:

$$-\dot{W} = \dot{m} (h_{02} - h_{01}) = \dot{m} \Delta h \quad (4.8)$$

Dividing by \dot{m} , it is seen that the enthalpy change over the compressor is in fact equal to the specific power input to the compressor required to bring the air from state 1 with temperature T_{01} and pressure p_{01} to state 2 with temperature T_{02} and pressure p_{02} . This observation is used in section (4.2.4) to identify what factors affect the enthalpy change.

4.2.3 Compressor Measurement Procedures

When the turbocharger is connected to the engine it is difficult to keep e.g. the shaft speed constant while investigating the dependence of pressure ratio on air mass flow. Therefore the stationary efficiency model for the compressor is based upon data from flow bench tests made by the manufacturer. A typical compressor map is shown in figure 4.3. Lines of constant compressor efficiency are superimposed in the same diagram as the speed lines.

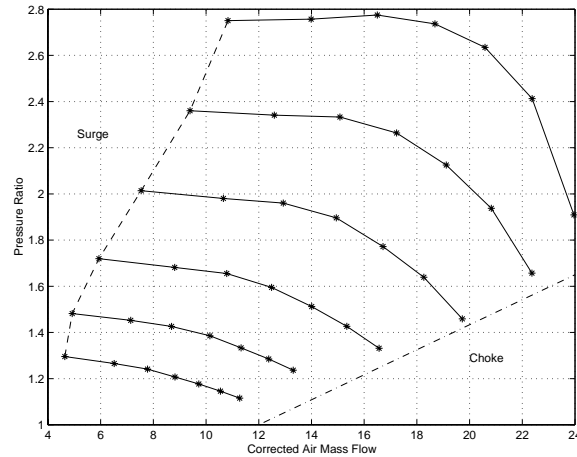


Figure 4.3 Typical compressor map. For each speedline there are two limits to the range of flow. The upper limit is due to choking, when the flow reaches the velocity of sound at some cross section. In this regime no further flow increase can be obtained by reducing the compressor outlet pressure and the speedline slope becomes infinite. The lower limit is due to a dangerous instability known as surge [13]. During surging a noisy and often violent flow process can occur causing cycle periods of back flow through the whole compressor and the installation downstream the compressor.

For validation purposes the following experiment was performed:

- \dot{m}_{air} , T_{af} , T_{comp} , p_{af} and p_{comp} were measured for different engine speeds and throttle plate positions.
- N ranges from 1500 rpm to 4500 rpm with steps of 500 rpm.
- α is varied in the entire engine working area.
- The parameters of interest were measured during 3 seconds and then averaged after waiting 10 seconds between each change in operating condition for stabilization of pressures.

correlation	U_c^2	U_c	$U_c \dot{m}_{air}$	\dot{m}_{air}^2	\dot{m}_{air}
Δh	0.9326	0.9278	0.6556	0.4272	0.4082

Figure 4.4 Correlations for enthalpy change over compressor.

4.2.4 Pressure Model

Using (4.6) together with (4.7) gives the following enthalpy change over the compressor;

$$\Delta h_{0c,s} = c_p \Delta T = c_p (T_{\text{comp}} - T_{\text{af}}) \quad (4.9)$$

Looking at the correlations with enthalpy given in table 4.4, supports this hypothesis as both U_c^2 and $U_c \dot{m}_{\text{air}}$, are highly correlated with Δh . Using this insight and adding \dot{m}_{air}^2 as a correction factor, a simple model for the enthalpy change is given by

$$\frac{\Delta h_{0c,s}}{c_p} = U_c^2 \left(s_1 \left(\frac{\dot{m}_{\text{air}}}{U_c} \right)^2 + s_2 \left(\frac{\dot{m}_{\text{air}}}{U_c} \right) + s_3 \right) \quad (4.10)$$

A least square fit gives the coefficients s_i . If (4.10) is put into (4.3), with the appropriate indices, a model for the pressure gain over the compressor for lower turbine shaft speeds is given;

$$\frac{p_{\text{comp}}}{p_{\text{af}}} = \left(1 + \frac{\Delta h_{0c,s}}{c_p T_{\text{af}}} \right)^{\frac{\gamma}{\gamma-1}} \quad (4.11)$$

The above enthalpy model was found simply by looking at the correlations, without requiring any physical insight. However the specific energy required for isentropic compression is given by subtracting the losses from the specific energy inputs;

$$\Delta h_{0c,s} = \Delta h_{0c} - \Delta h_{\text{loss}} \simeq \Delta h_{0c} - (\Delta h_{\text{frict}} + \Delta h_{\text{inc}}) \quad (4.12)$$

The level of specific energy input, Δh_{0c} , is proportional to the squared blade tip speed, and the dominant compressor losses, Δh_{loss} , stem from blade incidence losses and viscous friction. Friction loss is only mass flow dependant, whereas incidence loss also depends on compressor speed, hence all predictors in (4.10) could be explained by physical means.

Müller states that a successful model in general can not be constructed by independently modeling s_1 , s_2 and s_3 . In fact he finds that there is a physical relationship between s_1 and s_2 that should be utilized. By using the mass flow rate $\dot{m}_{\text{air,top}}$ for the maximum $\Delta h_{0c,s}$ Müller finds a dependence between coefficients and uses this dependence to implement the following model;

$$\left\{ \begin{array}{l} s_1 = s_{1,2} U_c^2 + s_{1,1} U_c + s_{1,0} \\ s_2 = \frac{2s_{1,2} \dot{m}_{\text{air,top}}}{U_c} \\ s_3 = s_{3,2} U_c^2 + s_{3,1} U_c + s_{3,0} \\ \text{with} \\ \dot{m}_{\text{air,top}} = m_2 U_c^2 + m_1 U_c + m_0 \end{array} \right.$$

As we have no possibility to calculate $\dot{m}_{\text{air,top}}$ with the data supplied to us from the manufacturer, we could not make any appropriate tests of this model. A slight suspicion though is that the main improvement that Müller found is due to the new set of regressors (U_c^4 , U_c^3 , $U_c^2 \dot{m}_{\text{air}}$, $U_c \dot{m}_{\text{air}}^2$ and \dot{m}_{air}) added to the model. As explained in appendix B.1 it is hazardous to introduce too many and highly correlated regressors.

To gain a better understanding of the compressor, a study of the velocity triangles is made. This gives the relationship between the enthalpies in (4.12). Velocity triangles at the entry, eye, and exit, tip, for the general case of the impeller with a prewhirl axial inducer and backsweep blades are shown in figure 4.5. The incoming air arrives at the impeller eye at an absolute velocity C_1 . Since the inlet velocity triangle at the eye hub will differ from that at the eye tip, a mean representative value must be considered, this will occur at the eye diameter that divides the eye into an annuli of equal area, D_1 . At this diameter the tangential velocity of the impeller is U_1 . The axial component of the absolute velocity, C_1 , of the air entering the inducer is C_{θ_1} , and the velocity relative to the inducer blade is W_1 . The optimal inlet angle is denoted β_{opt} . At the impeller tip the air leaves at an absolute velocity C_2 . The impeller tip speed is U_c , and the air velocity relative to the rotor blades is W_2 .

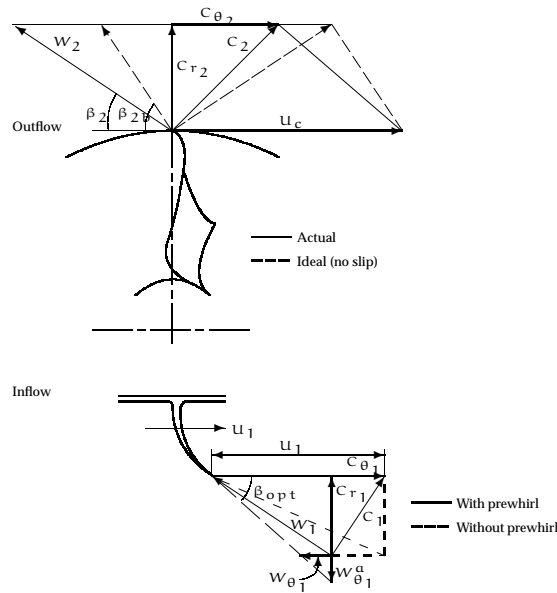


Figure 4.5 Velocity triangles for compressor (In most literature U_c is referred to as U_2).

Assuming that a separation of viscous friction losses into those stemming from the impeller and diffuser are not necessary, yields the following simple model for

friction losses.

$$\Delta h_{\text{frict}} = c_1 \dot{m}_{\text{air}}^{c_2} = \left[\text{choose } c_2 = 2 \right] = c_1 \dot{m}_{\text{air}}^2 \quad (4.13)$$

A simple model for incidence loss is presented in [13]. By assuming that kinetic energy loss is associated with the destruction of the tangential component of W_1 , as the fluid adapts to the blade direction, that is the tangential component $W_{\theta 1}$ which is the difference between actual incidence direction and ideal, the incidence energy losses are given by

$$\Delta h_{\text{inc}} = \frac{1}{2} W_{\theta 1}^2 \quad (4.14)$$

Looking at figure 4.5 and using some geometry gives

$$\begin{aligned} \frac{W_{\theta 1}^a + C_{r1}}{U_1 - C_{\theta 1}} &= \tan(\beta_{\text{opt}}) \\ \Rightarrow \\ W_{\theta 1}^a &= (U_1 - C_{\theta 1}) \tan(\beta_{\text{opt}}) - C_{r1} \end{aligned}$$

furthermore

$$W_{\theta 1} = W_{\theta 1}^a \cot(\beta_{\text{opt}}) = U_1 - C_{\theta 1} - C_{r1} \cot(\beta_{\text{opt}})$$

hence (4.14) could be formulated as:

$$\begin{aligned} \Delta h_{\text{inc}} &= \frac{1}{2} \left(U_1 - C_{\theta 1} - C_{r1} \cot(\beta_{\text{opt}}) \right)^2 = \\ &= \frac{1}{2} \left(U_1^2 - 2U_1 C_{r1} \cot(\beta_{\text{opt}}) + C_{r1}^2 \cot^2(\beta_{\text{opt}}) + \right. \\ &\quad \left. + C_{\theta 1} (C_{\theta 1} - 2U_1 + 2C_{r1} \cot(\beta_{\text{opt}})) \right) \end{aligned}$$

Compressors with axial inlet flow have no inlet prewhirl in the ideal case. Assuming that conditions are close to ideal the inlet prewhirl is set to zero, $C_{\theta 1} = 0$;

$$\Delta h_{\text{inc}} = \frac{1}{2} \left(U_1^2 - 2U_1 C_{r1} \cot(\beta_{\text{opt}}) + C_{r1}^2 \cot^2(\beta_{\text{opt}}) \right) \quad (4.15)$$

The ideal enthalpy change is given by;

$$\Delta h_{0c} = \frac{\dot{W}}{\dot{m}_{\text{air}}} = U_c C_{\theta 2} = U_c^2 \left(1 - \frac{C_{r2}}{U_c} \cot(\beta_{2b}) \right) \quad (4.16)$$

Moreover the absolute velocity of the air leaving the impeller tip is given by

$$C_{r1} = \frac{\dot{m}_{\text{air}}}{\rho_1 A_1}$$

where A_1 is the inducer inlet cross sectional area and ρ_1 is the compressor inlet static density. Furthermore U_1 is related to U_c as the D_1 is related to the impeller tip diameter D_2 ;

$$\frac{U_1}{U_c} = \frac{D_1}{D_2}$$

Using the equalities above and inserting (4.13), (4.15) and (4.16) into (4.12), and after some algebraic manipulation and identification with (4.10) it gives;

$$\begin{cases} \frac{s_1}{c_p} = -\left(\frac{\cot(\beta_{opt})}{\rho_1 A_1}\right)^2 + k_2 = k_1^2 + k_2 \\ \frac{s_2}{c_p} = \frac{D_1}{D_2} \left(\frac{\cot(\beta_{opt})}{\rho_1 A_1}\right) = k_1 k_3 \end{cases}$$

Using the relationship between s_1 and s_2 the following model may now be formulated;

$$\frac{\Delta h_{0c,s}}{c_p} = U_c^2 \left((k_1^2 + k_2) \left(\frac{\dot{m}_{air}}{U_c}\right)^2 + k_1 k_3 \left(\frac{\dot{m}_{air}}{U_c}\right) + k_4 \right) \quad (4.17)$$

where k_i are constants. As can be seen both (4.10) and (4.17) have the same predictors and degree of freedom. The difference is that the latter one was derived from physical relationships. Either of the two models may be used with the same result, but as (4.10) has less coefficients it is to prefer.

Figure 4.6 shows validation data for (4.10). The model has an average error of around 3.65%. Note that for very small pressure losses, relative errors may become very large due to division by a small number. If the relative error is calculated for the pressure ratio instead this problem is avoided. Such an approach gives an average error < 0.5%, which is also the case for pressure models presented in previous chapters.

4.2.5 Efficiency Model

Looking at figure 4.2 it is clear that the isentropic and ideal enthalpy change has the same characteristics, and as described in section 4.2.2 the efficiency is defined by the ratio between the two enthalpies, see equation (4.4). Using equation (4.10) for the isentropic enthalpy change and dividing with the real enthalpy changed, modeled by

$$\Delta h_{0c} = b_1 \dot{m}_{air} + b_2 \dot{m}_{air} U_c + b_3 U_c^2 + b_4 U_c + b_5$$

gives the following nonlinear model for the efficiency

$$\eta_{C,TS} = \frac{\Delta h_{c,s}}{\Delta h_{0c}} = \frac{U_c^2 \left(s_1 \left(\frac{\dot{m}_{air}}{U_c}\right)^2 + s_2 \left(\frac{\dot{m}_{air}}{U_c}\right) + s_3 \right)}{b_1 \dot{m}_{air} + b_2 \dot{m}_{air} U_c + b_3 U_c^2 + b_4 U_c + b_5} \quad (4.18)$$

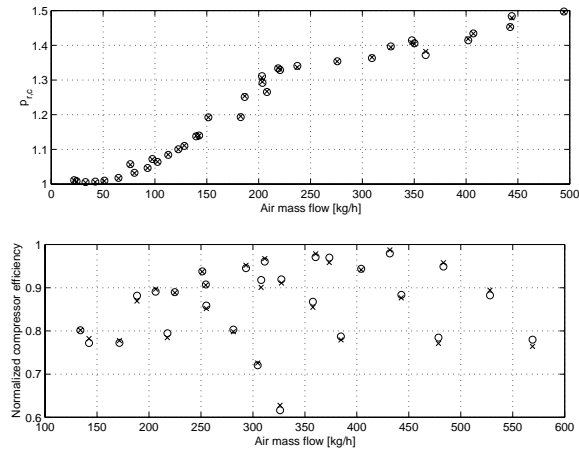


Figure 4.6 'x' denotes actual value and 'o' model value. The upper figure shows validation of pressure model. Validation for these model is based on experiments on Vehicular Systems engine, while the bottom figure, which shows validation of normalized efficiencies for speedlines up to 140000 rpm, is validated with data supplied by the manufacturer.

Fitting this model to the speed lines up to 140000 rpm gives an average error of 0.89% and a maximum error of 2.25% in this region (see figure 4.6).

It could be reasoned that a model with the same parameterization for the isentropic as for the real enthalpy change, with different constants, should give a good model for the efficiency. Nevertheless this approach was not successful. It should be noted that this model is pretty complex, and therefore it is of great interest to further develop it. It might be a good idea to use a performance map instead of (4.18).

4.2.6 Compressor Summary

$$\frac{\Delta h_{0c,s}}{c_p} = 10^{-5} u_c^2 \left(s_1 \left(\frac{\dot{m}_{air}}{u_c} \right)^2 + s_2 \left(\frac{\dot{m}_{air}}{u_c} \right) + s_3 \right)$$

$$u_c = \frac{N_t}{60} D_2$$

$$p_{r,c} = \frac{p_{comp}}{p_{af}} = \left(\frac{\Delta h_{0c,s}}{c_p T_{af}} + 1 \right)^{\frac{\gamma}{\gamma-1}}$$

$$\eta_{C,TS} = \frac{u_c^2 \left(s_1 \left(\frac{\dot{m}_{air}}{u_c} \right)^2 + s_2 \left(\frac{\dot{m}_{air}}{u_c} \right) + s_3 \right)}{b_1 \dot{m}_{air} + b_2 \dot{m}_{air} u_c + b_3 u_c^2 + b_4 u_c + b_5}$$

4.3 Turbine

The flowing exhaust gases propels the turbine, which via the turbine shaft delivers power to the compressor. In this section models for exhaust expansion ratio and the turbine isentropic efficiency will be developed. These are used later on in section 4.4 together with the compressor models to calculate an expression for the turbine shaft speed.

4.3.1 Physical Relationships for the Turbine

The turbine works in the same way as the compressor, only in the reverse mode. Thus the physical relationships in section (4.2) is valid for the turbine too but is repeated here for convenience, with the correct indication. The expression for the expansion ratio is:

$$\frac{p_4}{p_3} = \left(\frac{T_{4, is}}{T_3} \right)^{\frac{\gamma}{\gamma-1}}$$

where 3 and 4 denotes inlet and outlet respectively. As for the compressor, a measure of the efficiency is introduced to account for deviation from an isentropic process. For the turbine it is defined as the actual work output divided by that from a reversible isentropic expansion between the same two values of the pressure:

$$\eta_t = \frac{\text{actual work}}{\text{isentropic work}}$$

Again this definition can be stated in two versions depending on whether or not the kinetic energy in the final state can be utilized. If that is the case, use η_{tTT} , if not use η_{tTS} . Only the latter definition is printed out since it is the most realistic and most commonly used.

$$\eta_{tTS} = \frac{h_{03} - h_{04}}{h_{03} - h_{4s}} = [c_p = \text{constant}] = \frac{T_{03} - T_{04}}{T_{03} - T_{4s}} = \frac{-\Delta T}{-\Delta T_{is}} \quad (4.19)$$

In order for the last equality to be valid, the specific heat c_p for the exhaust gas must be considered as a constant. However in the temperature range of interest c_p may vary significantly, so that c_p is taken as the mean value of that at temperature T_3 and T_4 .

$$\frac{p_4}{p_3} = \left(1 + \frac{\Delta T}{T_3} \right)^{\frac{\gamma}{\gamma-1}} \quad (4.20)$$

4.3.2 Turbine Measurement Procedures

There are situations when it is desirable to reduce the compression ratio of the intake air. For example, when the engine is not running at full load, and the throttle

plate is only partially open, the largest portion of the total pressure loss in the entire intake system is due to the passage past the throttle plate. Therefore no positive effect is accomplished by compressing the air in this case. Another scenario is that the turbocharger is supplied with too high exhaust air mass flow and will overspeed. To accomplish this reduction in the pressure ratio, some amount of the exhaust gas is passed by the turbine to the exhaust pipe, reducing the turbine shaft speed and thus the power supplied to the compressor. The bypass valve or *waste gate* is governed by a controller so that the portion of the exhaust gases that flow through to the turbine can be controlled in a way that enables safe engine operation.

As the actual mass flow through the turbine can not be measured in the laboratory, it is desirable to disengage the wastegate in order to calculate correct models. However, this is not done in this project, instead data supplied by the manufacturer is used to develop the pressure and efficiency models below.

4.3.3 Turbine Isentropic Efficiency Model

Using the total to static efficiency definition in 4.19 and, with the same reasoning as for the compressor, modeling the isentropic and the real enthalpy change respectively, the following expression for the turbine isentropic efficiency is found:

$$\eta_{t,TS} = \frac{U_t^2 \left(s_1 \left(\frac{\dot{m}_{turbine}}{U_t} \right)^2 + s_2 \left(\frac{\dot{m}_{turbine}}{U_t} \right) + s_3 \right)}{b_1 \dot{m}_{turbine} + b_2 \dot{m}_{turbine} U_t + b_3 U_t^2 + b_4 U_t + b_5} \quad (4.21)$$

This model gives an average error of 0.41% and maximum error of around 1.0% for manufacturers data for the four lower speed lines (Shaft speeds below 140000 rpm). As no appropriate tests could be done at our test bench a validation figure is not presented. However the same remarks on model complexity as for the compressor efficiency are valid, see section 4.2.5.

4.3.4 Pressure Model

As figure 4.7 shows, it exists a nearly linear relationship between mass flow and pressure ratio for the turbine. And the relation is practically independent of turbine shaft speed. That is the following model should be suitable;

$$p_{r,t} = \frac{p_{turbine}}{p_{exh}} = 1 + r_2 \dot{m}_{turbine}^2 + r_1 \dot{m}_{turbine} \quad (4.22)$$

To make the model more general, volume flow should be considered instead of mass flow as explained in earlier sections, but as we do not know the molar gas constant, R , for the exhaust gases this is not done. The resulting model (4.22) has an average error less than 1.5%.

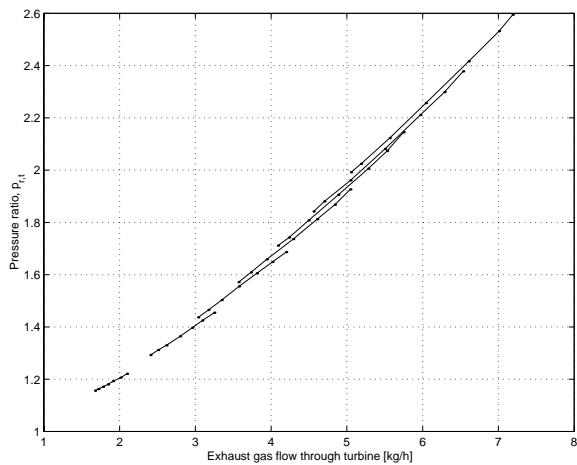


Figure 4.7 Pressure ratio plotted versus mass flow for different turbine shaft speeds. Note that the relationship is almost speed independent of the shaft speed.

4.3.5 Turbine Summary

$$\eta_{t,TS} = \frac{\Delta h_{t,s}}{\Delta h_{0t}} = \frac{U_t^2 \left(s_1 \left(\frac{\dot{m}_{\text{turbine}}}{U_t} \right)^2 + s_2 \left(\frac{\dot{m}_{\text{turbine}}}{U_t} \right) + s_3 \right)}{b_1 \dot{m}_{\text{turbine}} + b_2 \dot{m}_{\text{turbine}} U_t + b_3 U_t^2 + b_4 U_t + b_5}$$

$$U_t = \frac{N_t}{60} D_{2,t}$$

$$p_{r,t} = 1 + r_2 \dot{m}_{\text{turbine}}^2 + r_1 \dot{m}_{\text{turbine}}$$

4.4 Turbo Dynamics

4.4.1 Turbine Shaft Speed

In the previous sections models for the compression ratio and the expansion ratio for the compressor and the turbine respectively, were developed. In order to connect the two submodels, a relation describing the turbine shaft speed is needed. For this purpose the following balance equation, expressing the conservation of energy, is used:

$$\text{Produced power} - \text{Consumed power} = \text{Stored energy per unit of time}$$

Applying this to the turbo charger gives:

$$\frac{d}{dt}E = \dot{W}_{\text{prod}} - \dot{W}_{\text{cons}} \quad (4.23)$$

where \dot{W}_{prod} and \dot{W}_{cons} denotes the power produced by the turbine and the power consumed by the compressor respectively and E is the energy stored in the rotating parts of the turbo charger.

If the turbine and the compressor is treated as two separate thermodynamic systems, \dot{W}_{prod} and \dot{W}_{cons} can be calculated from the first law of thermodynamics, as stated in appendix B.2. Again the heat transfer with the surroundings and change in potential energy is neglected.

$$-\dot{W} = \dot{m}(h_{02} - h_{01}) = \dot{m}c_p(T_{\text{out}} - T_{\text{in}}) = \dot{m}c_p\Delta T \quad (4.24)$$

Starting with the calculations for the compressor for which the net amount of produced power is negative, i.e. the compressor consumes energy, that is $\dot{W}_{\text{cons}} = -\dot{W}$, equation (4.6) can be rearranged to express temperature change in terms of pressure ratio.

$$\Delta T = \frac{T_{\text{af}}}{\eta_c} \left(\left(\frac{p_{\text{comp}}}{p_{\text{af}}} \right)^{\frac{\gamma_c - 1}{\gamma_c}} - 1 \right)$$

so that equation (4.24) takes the form:

$$\dot{W}_{\text{cons}} = \dot{m}c_{p,c}T_{\text{af}} \frac{1}{\eta_c} \left(\left(\frac{p_{\text{comp}}}{p_{\text{af}}} \right)^{\frac{\gamma_c - 1}{\gamma_c}} - 1 \right) \quad (4.25)$$

For the turbine, the net amount of produced energy is positive and thus $\dot{W}_{\text{prod}} = \dot{W}$. From equation (4.20):

$$\Delta T = T_{\text{exh}}\eta_t \left(\left(\frac{p_{\text{turbine}}}{p_{\text{exh}}} \right)^{\frac{\gamma_t - 1}{\gamma_t}} - 1 \right)$$

Finally, the expression for the produced energy becomes:

$$-\dot{W}_{\text{prod}} = \dot{m}_t c_{p,t} T_{\text{exh}} \eta_t \left(\left(\frac{p_{\text{turbine}}}{p_{\text{exh}}} \right)^{\frac{\gamma_t-1}{\gamma_t}} - 1 \right) \quad (4.26)$$

The stored energy, E , for a rigid body rotating with angular velocity ω about a fixed axis is:

$$E = \frac{I\omega^2}{2}$$

where I is the moment of inertia with respect to the axis of rotation and is constant for the specific body studied. Differentiating this relation with respect to time gives the stored energy per unit of time:

$$\frac{d}{dt} \left(\frac{I\omega(t)^2}{2} \right) = I\omega(t)\dot{\omega}(t) \quad (4.27)$$

Inserting (4.26), (4.25), (4.27) in (4.23), the final expression for the turbine shaft speed model becomes

$$\begin{aligned} I\omega\dot{\omega} = & \dot{m}_t c_{p,t} T_{\text{exh}} \eta_t \left(\left(1 - \frac{p_{\text{turbine}}}{p_{\text{exh}}} \right)^{\frac{\gamma_t-1}{\gamma_t}} \right) - \\ & - \dot{m}_c c_{p,c} T_{\text{af}} \frac{1}{\eta_c} \left(\left(\frac{p_{\text{comp}}}{p_{\text{af}}} \right)^{\frac{\gamma_c-1}{\gamma_c}} - 1 \right) \end{aligned}$$

Note that in the above expression it is assumed that the turbo charger friction is included in either η_t or η_c , otherwise the power loss by friction must be included explicitly. The shaft speed equation can be converted to express the dynamic behavior in terms of revolutions per minute, rather than radians per second, by using the following relation:

$$N_t = \frac{60\omega}{2\pi}$$

4.4.2 Turbine Shaft Speed Summary

$$I\omega\dot{\omega} = \dot{W}_{\text{prod}} - \dot{W}_{\text{cons}}$$

$$\dot{W}_{\text{prod}} = \dot{m}_t c_{p,t} T_{\text{exh}} \eta_t \left(\left(1 - \frac{p_{\text{turbine}}}{p_{\text{exh}}} \right)^{\frac{\gamma_t - 1}{\gamma_t}} \right)$$

$$\dot{W}_{\text{cons}} = \dot{m}_c c_{p,c} T_{\text{af}} \frac{1}{\eta_c} \left(\left(\frac{p_{\text{comp}}}{p_{\text{af}}} \right)^{\frac{\gamma_c - 1}{\gamma_c}} - 1 \right)$$

Conversion from $\frac{\text{rad}}{\text{s}}$ to rpm :

$$N_t = \frac{60\omega}{2\pi}$$

Remark: The turbo charger friction is assumed to be included in either η_t or η_c .

Chapter 5

Engine

In this chapter the standard models for fuel dynamic, engine torque and engine inertia are presented briefly. This is done to get a picture of how the engine operates. However only a model for the injected fuel at stationary conditions is completely developed and validated. For a more thorough presentation please refer to Nielsen and Eriksson [19].

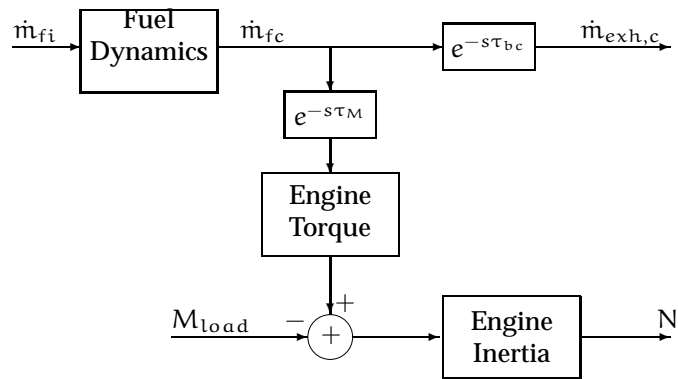


Figure 5.1 Schematic picture of the subsystems that are included in this chapter.

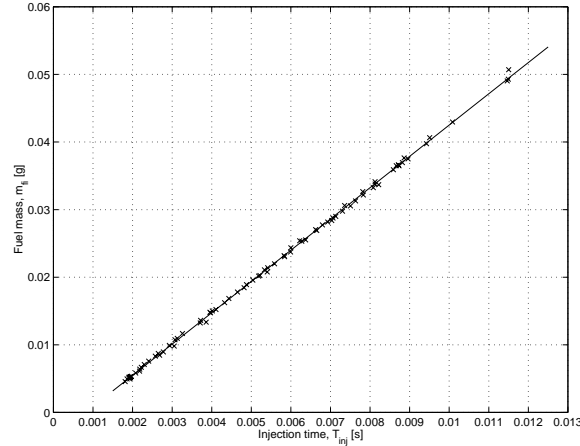


Figure 5.2 Fuel mass in to one cylinder as function of injection time. 'x' marks measured values and the line marks model values.

5.1 Fuel Dynamics

Fuel is injected to the engine just before the inlet valve and enters the cylinder together with the air when the intake valve is opened. The amount of fuel injected is given by the fuel injection time as described below. However not all of the injected fuel is inducted immediately to the engine as some of it is deposited in the intake either as a film or as a puddle. This phenomenon is referred to as *wall wetting* and has been proposed as for partly explaining the dynamic response from a step in fuel injection time, t_{inj} , to the measured λ (the other part of the explanation is the dynamic in the sensor).

5.1.1 Fuel Injection

The fuel flow into the cylinder is governed by an electrically controlled valve. The fuel injector opens one time each revolution, and the closing time for the injector is usually timed to occur before the inlet valve opening. The amount of fuel injected is proportional to the injection valve opening time, t_{inj} , less a lumped opening and closing time. The opening and closing times of the valve, t_0 , depend on the battery voltage, u_{batt} , since the opening of the valve depends on the current through the solenoid that opens it. When the current is shut off the valve is closed by a spring.

$$m_{fi} = c(t_{inj} - t_0(u_{batt})) \quad (5.1)$$

Averaging the injected fuel over a cycle and multiplying with the engine speed, yields the fuel flow.

$$\dot{m}_{fi} = N m_{fi} = N c(t_{inj} - t_0(u_{batt}))$$

Figure 5.2 shows a validation of how good the model approximates the inducted fuel.

5.1.2 Wall Wetting

A popular description of the fuel dynamics due to wall wetting is given by Aquino [21]. When fuel is injected some fraction X of it is deposited on the wall and forms a fuel film (some times also called fuel puddle), while the rest $(1 - X)$, mixes with the air. Evaporation is assumed to be proportional to the area of the film, which in turn is assumed to be proportional to the mass in the film, m_{fp} . The change in this fuel puddle mass is the deposited mass, $X\dot{m}_{fi}$ minus the mass evaporated from the puddle, $\frac{1}{\tau_{fp}}m_{fp}$:

$$\frac{dm_{fp}}{dt} = X\dot{m}_{fi} - \frac{1}{\tau_{fp}}m_{fp}$$

The fuel flow into the cylinder, \dot{m}_{fc} , is the sum of the part that goes directly from injection, $(1 - X)\dot{m}_{fi}$, and the part that is evaporated, $\frac{1}{\tau_{fp}}m_{fp}$:

$$\dot{m}_{fc} = (1 - X)\dot{m}_{fi} + \frac{1}{\tau_{fp}}m_{fp}$$

Both X and τ depend on the engine state as well as fuel properties. That is even though everything around the engine is kept constant, the parameters still change with operating condition. This is due to the fact that evaporation depends on the air flow passing the deposits. A simple model for this is to let the parameters be stationary functions of operating point (N, p_{man}) . If experiments are performed to map X and τ and models are developed for them the above expressions may be used to calculate the (A/F) mixture that enters the cylinder:

$$\lambda = \frac{\dot{m}_{air,c}}{\dot{m}_{fc}} \frac{1}{(A/F)_s} \quad (5.2)$$

5.1.3 Fuel Dynamics Summary

$$\dot{m}_{fi} = c_0 N (t_{inj} - \tau_0)$$

5.2 Engine Torque

The torque is a measure of an engine's ability to do work and is normally measured with a dynamometer; power is the rate at which work is done. It follows that the power P delivered by the engine and absorbed by the dynamometer is the product of torque and angular speed:

$$P = 2\pi NT \quad (5.3)$$

where N is the crankshaft rotational speed. Ideally all the heat stored in the fuel may be converted to power, that is the delivered power is given by taking the product of the heating value of the fuel, $Q_{\text{fuel}} = Q_{\text{H.V.}} = 47$ [MJ/kg] for isoctane, and the fuel mass flow through the cylinders, \dot{m}_{fc} . However there will be losses during the energy conversion, thus we have to multiply with the fuel conversion efficiency, η_f :

$$P = Q_{\text{fuel}}\eta_f\dot{m}_{\text{fc}} \quad (5.4)$$

Finally if (5.3) and (5.4) are combined a model for the engine torque is given:

$$T = \frac{Q_{\text{fuel}}\eta_f\dot{m}_{\text{fc}}}{2\pi(N/60)} = \mathcal{T} \frac{\dot{m}_{\text{fc}}}{N} \quad (5.5)$$

where the constant \mathcal{T} is found by a least square fit.

5.3 Engine Inertia

The driving torque from combustion, M_{comb} , depends on the operating conditions, the air/fuel ratio, and the ignition timing. The rotational dynamics for the crank shaft is given by Newton's second law by subtracting the friction torque, M_{fric} , and external load from the vehicle, M_{load} , from M_{comb} :

$$J \frac{dw}{dt} = M_{\text{comb}}(p_{\text{man}}, N, \lambda, \theta_{\text{ig}}) - M_{\text{fric}}(N, p_{\text{man}}) - M_{\text{load}}$$

The combustion and friction torques can be lumped together to M_e and when not considering variations in the spark advance, θ_{ig} , this yields the following equation for the crank shaft model

$$\frac{dN}{dt} = C \cdot (M_e(p_{\text{man}}, N, \lambda) - M_{\text{load}}) \quad (5.6)$$

If the time delay, τ_M , from the time that fuel is injected to that when torque contribution can be detected at the crank shaft is considered, an experiment may be performed to find the constant C .

Chapter 6

Summary

6.1 Conclusions

A structure for an MVEM, consisting of several submodels, suitable for the stationary case is developed. Pressures, temperatures, efficiencies, rotational speeds and gas mass flows, are used to interconnect the submodels. Stationary models for most of these, namely the air filter, intercooler, throttle, engine, compressor, and turbine, is then developed and summarized.

To get as general models as possible, most models are based on well known physical relationships, with appropriate simplifications made, but when this approach fails, or is insufficient, black box models are used. These models are found by using the theory for multiple regression. The dynamic behavior for the intake manifold and turbine shaft speed is studied and modeled.

Except for the turbine and turbine shaft models, that can not be validated due to limited control over the exhaust gas flow through the turbine, all the validated models have a relative mean error below 2%, which is a satisfying result.

6.2 Future Work

The stationary models on the the turbo charger, waste gate and catalyst, should be further developed and tested for dynamic data. It is also desirable to get a better knowledge and understanding of the temperature behavior, especially on the exhaust side. Furthermore it is of great interest to develop models for the dynamic behavior of all components, and for completeness a study of how ambient condi-

tions affect the system is needed. When this is done an exciting possibility would be to implement all the submodels in one or several suitable simulation environments, such as Simulink, Modelica or Dymola and develop a model library. These models may then be used as stand alone components for simulation, control, or diagnosis purposes, or interconnected to each other to form a complete Mean Value Engine Model.

Bibliography

[Thermodynamics]

- [1] Kittel, C., Kroemer, H., *Thermal physics 2nd ed.*, Freeman, 1980, ISBN 0-7167-1088-9
- [2] Jones, J.B., Dugan, R.E., *Engineering Thermodynamics*, Prentice Hall, Englewood Cliffs, 1996, ISBN 0-02-361332-7
- [3] Van Wylen, G., Sonntag, R., Borgnakke, C., *Fundamentals of Thermodynamics*, 4th ed., John Wiley & Sons, Inc., 1994, ISBN 0-471-59395-8
- [4] Schmidt, F.W., Henderson, R.E., Wolgenmuth, C.H., *Introduction to Thermal Sciences: thermodynamics, fluid dynamics, heat transfer*, 2nd ed., John Wiley & Sons, Inc., 1993, ISBN 0-471-54939-8

[Heat Transfer]

- [5] Holman, J.P., *Heat Transfer, 7th ed, in SI units*, McGraw-Hill, 1992, ISBN 0-07-112644-9
- [6] Baehr H.D., Stephan, K., *Heat and Mass Transfer*, Springer, 1998, ISBN 3-540-63695-1

[Fluid Mechanics]

- [7] Appelqvist, B., Loyd, D., *Grundläggande Teknisk Strömningslära*, Ingenjörsför, 1979, ISBN 91-7284-092-7

[8] Nakayama, Y., Boucher, R.F., *Introduction to Fluid Mechanics*, Arnold, 1999, ISBN 0-340-67649-3

[9] Franzini, J.B., Finnemore, E.J.; *Fluid Mechanics, 9th ed*, WCB/McGraw-Hill, 1997, ISBN 0-07-114214-2

[Fundamentals of Control and Modeling]

[10] Levine, W.S., *The Control Handbook*, CRC Press, Inc., 1996, ISBN 0-8493-8570-9

[11] Ljung, L., *Modeling of Dynamic Systems*, Prentice Hall, 1994, ISBN 0-13-597097-0

[Mean Value Engine Modeling]

[12] Heywood, J.B., *Internal Combustion Engine Fundamentals*, McGraw-Hill, 1988, ISBN 0-07-100499-8

[13] Watson, N., Janota, M.S., *Turbocharging the Internal Combustion Engine*, The Macmillan Press Ltd, 1982, ISBN 0-333-24290-4

[14] Moraal, P., Kolmanovsky, I., *Turbocharger Modeling for Automatic Control Applications*, Society of Automotive Engineers, Inc., 1999, SAE 1999-01-0908 (SP-1451)

[15] Müller, M., Hendricks, E., Sörenson, S.C., *Mean Value Modeling of Turbocharged Spark Ignition Engines*, Society of Automotive Engineers, Inc., 1998, SP-1330

[16] Fons, M., Sorenson, S.C., Hendricks, E., Vigild, C., Chevalier A., *Mean Value Engine Modeling of an SI Engine with EGR*, Society of Automotive Engineers, Inc., 1999, SAE 1999-01-0909 (SP-1451)

[17] Hendricks, E., Chevalier, A., Jensen, M., Sörenson, S.C., *Modeling of the Intake Manifold Filling Dynamics*, Society of Automotive Engineers, Inc., 1996, 960037 (SP-1149)

[18] Hendricks, E., Vesterholm, T., Sörenson, S.C., *Nonlinear, Closed Loop, SI Engine Control Observers*, Society of Automotive Engineers, Inc., 1992, SAE 920237 (SP-898)

[19] Nielsen, L., Eriksson, L., *Course material Vehicular Systems*, Linköping Institute of Technology, 1999, Linköping

[20] Nyberg, M., *Model Based Fault Diagnosis -Methods, Theory, and Automotive Engine Applications*, Linus & Linnea AB, 1999, ISBN 91-7219-521-5

[21] Aquino, C., *Transient A/F control characteristics of the 6 liter central fuel injection engine*, Society of Automotive Engineers, Inc., 1981, SAE 810494

- [22] Hires, S., Overington, M., *Transient mixture strength excursions - an investigation of their causes and the development of a constant mixture strength fueling strategy*, Society of Automotive Engineers, Inc., 1981, SAE 810495 (SP-487)
- [23] Olin, P.M., Maloney, J.M., *Barometric Pressure Estimator for Production Engine Control and Diagnostics*, Society of Automotive Engineers, Inc., 1999, SAE 1999-01-0206, (SP-1418)
- [24] Guzzella, L., Amstutz, A., *Control of Diesel Engines*, IEEE Control Systems Society, 1998, 0272-1708/98

[Regression Analysis]

- [25] Enqvist, E. *Grundläggande regressionsanalys, . . .*
- [26] Draper, N.R., *Applied Regression Analysis, 2nd ed*, Wiley, 1981, ISBN 0-471-02995-5
- [27] Weisberg, S., *Applied Linear Regression, 2nd ed*, Wiley, 1985, ISBN 0-471-87957-6

[Optimization]

- [28] Luenberger, D.G., *Linear and Nonlinear Programming*, Addison-Wesley, ISBN 0-201-15794-2

Appendix A

The System

Engine Specifications The engine is a standard Saab 2.3 liter SI engine with low pressure exhaust turbo charger equipped with extra sensors for measurements of pressure, temperatures, etc.

Engine type:	Saab B235E
Cylinders:	4
Firing order:	1-3-4-2
Valves:	16
Displacement:	2.3 liters
Bore:	90 mm
Stroke:	90 mm
Compression ratio $r_c = \frac{V}{V_c}$	9.3
Maximum Engine Power:	125 kW
Maximum Engine Torque:	210 Nm

Brake DYNAS₂. Maximum effect 220 kW. The brakes torque and speed can be read manually or through VXI.

VXI HP-VXI¹ One HP8491A controller, one HP1433 for fast collection of data (8 channels, 196 kSampels/s per channel) and a slower module HPE1415A (32 channels, 2.5 kSampel/s per channel).

¹VME bus eXtensions for Instrumentation. VME is an industrial standard for instruments.

Trionic T7 Engine system.

App7 Software that uses CAN² i used to read parameters in the engine system Trionic.

²Controller Area Network

Appendix B Theory

In this appendix some of the theory needed to understand this master thesis is presented. This should be a repetition from undergraduate courses. References to appropriate literature is given in each section.

B.1 Multiple Linear Regression

A rather simple approach for modeling, without having full physical insight, is to use multiple linear regression, which is a standard method presented in most fundamental courses in statistics for undergraduate level. A brief introduction to this method is given below.

Assume we have input signals x_1, x_2, \dots, x_k , and an output signal y . If the absolute value of the correlation between x_i and y is close to 1, then multiple linear regression might be a good way to find a suitable model. In the general case it is desired to explain the variations in the response variable y using a number of predictors x_1, x_2, \dots, x_k . If we formulate the following relation

$$y = a_0 + a_1x_1 + a_2x_2 + \dots + a_kx_k$$

and then collect observed data:

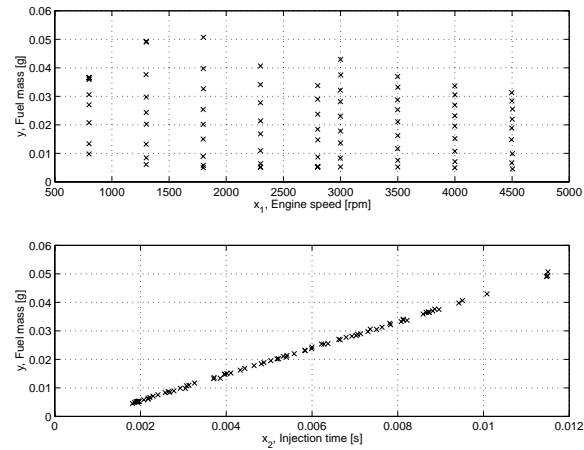
$$(x_{11}, x_{12}, \dots, x_{1k}, y_1), (x_{21}, x_{22}, \dots, x_{2k}, y_2), \dots, (x_{n1}, x_{n2}, \dots, x_{nk}, y_n)$$

this may be used together with the Least Squares Method (LSM) to calculate the coefficients $a_0, a_1, a_2, \dots, a_k$, that gives the model. It should be noted that by adding more predictors a better fit to collected observed data may be found, but a great hazard by doing this is that the model might lose extrapolating capabilities and thus generality. In other words the model will be very well suited to “predict” the already observed data, but bad at predicting new data. Several tests have been developed to decide if a predictor should be accepted or not, but are not presented here. For a more thorough description, see e.g. [25], [26], or [27]. Below a very basic example on multiple linear regression follows.

Example B.1 *To develop a model for the amount of fuel injected to a cylinder an experiment was performed. During the experiment the following parameters were measured:*

$$\begin{aligned} y &= \text{fuel mass, } m_{fi} \\ x_1 &= \text{engine speed, } N \\ x_2 &= \text{fuel injection time, } t_{inj} \end{aligned}$$

Thereafter y was plotted versus x_1 and x_2 :



It is obvious from the figures that x_1 is a bad predictor for y , while x_2 is very good. This is also illustrated by looking at correlations:

$$\begin{array}{rcc} & y & x_1 \\ x_1 & -0.2178 & \\ x_2 & 0.9998 & -0.2179 \end{array}$$

Thus it should be interesting to describe the injected engine fuel as a function of the fuel injection time;

$$\begin{aligned} y &= a_1 x_2 + a_0 \\ \text{or} \\ m_{fi} &= a_1 t_{inj} + a_0 \end{aligned}$$

This is actually done in section 5.1.1 and the resulting model is validated in figure 5.2.

B.2 Thermodynamics

On most undergraduate courses thermodynamics is presented from a statistical point of view (This approach is taken by e.g. Kittel [1]). A more engineering directed approach though is taken by e.g. Van Wylen, Sonntag and Borgnakke [3] and Jones and Dugan [2], where thermodynamics is looked into from a macroscopic perspective. The latter book gives a very well structured and easy to read presentation of thermodynamics and is highly recommended.

Thermodynamics is the science of energy. A thermodynamic system is defined as any quantity of matter or any region of space to which we direct attention for purpose of analysis. The quantity of matter or region of space must be within the prescribed boundary. This boundary may be deformable or rigid; it may even be imaginary. Thermodynamics is characterized by a few basic principles, stated as postulates below.

Zerth law If two systems are in equilibrium with a third system, they must be in internal equilibrium with each other.

First law For any cycle of a closed system, the net heat transfer equals the net work;

$$\oint \delta Q = \oint \delta W \quad (\text{B.1})$$

This law is no more than a statement of the principle of conservation of energy.

Second law (Clausius statement) The second law has been stated in many different forms. However, if any one of the statements is accepted as a postulate, all the other statements can be proved from this starting point. We shall use Clausius statement; It is impossible for any device to operate in such a manner that it produces no effect other than the transfer of heat from one body to another body at higher temperature.

Third law As the temperature of a pure substance approaches zero on the Kelvin scale, the entropy of the substance approaches zero. Note that there are important restrictions on the third law as stated here. However the important result is that the third law makes it possible to determine absolute entropies.

The laws of thermodynamics are supported by a vast number of experiments; no exceptions have been observed. Consequently, we accept them as laws of nature.

B.2.1 Steady Flow System

A common assumption when analyzing thermodynamic systems is to say that the fluid flow is steady and one-dimensional. If velocity, temperature, pressure and other properties are uniform at each cross section flow is said to be one-dimensional. From one cross section to another the properties may change, but for each value of the coordinate (defined as distance in the direction of flow) there is a single value of velocity, a single value of density and so on. Moreover, for a steady-flow system all fluid properties must be independent of time. From this definition the following necessary and sufficient conditions for a steady flow system may be stated:

1. The properties of the fluids crossing the boundary remain constant at each point on the boundary.
2. The flow rate at each section where matter crosses the boundary is constant.
3. The rate of mass flow into the system equals the rate of mass flow out. Consequently, the amount of mass within the system is constant.
4. The volume of the system remains constant. The system boundary must be rigid.
5. All interactions with the surroundings occur at a constant rate.

For the frequently encountered case of a single inlet and a single outlet the *continuity equation*, an equation that simply expresses the conservation of mass under steady flow conditions, becomes

$$\dot{m} = \rho_1 V_1 A_1 = \rho_2 V_2 A_2$$

where the subscript 1 denotes inlet conditions and 2 outlet conditions, ρ is the density and V velocity of the fluid, and A is the opening area at inlet and outlet respectively.

B.2.2 Applied Thermodynamics for MVEM

For MVEM purposes the most interesting law is the first law statement, (B.1), which is an energy balance;

$$\left(\begin{array}{c} \text{Net} \\ \text{increase} \\ \text{in stored} \\ \text{energy of} \\ \text{system} \end{array} \right) = \left(\begin{array}{c} \text{Net amount of} \\ \text{energy added to} \\ \text{system as heat} \\ \text{and all forms of} \\ \text{work} \end{array} \right) + \left(\begin{array}{c} \text{Stored} \\ \text{energy} \\ \text{of matter} \\ \text{entering} \\ \text{system} \end{array} \right) - \left(\begin{array}{c} \text{Stored} \\ \text{energy} \\ \text{of matter} \\ \text{leaving} \\ \text{system} \end{array} \right) \quad (\text{B.2})$$

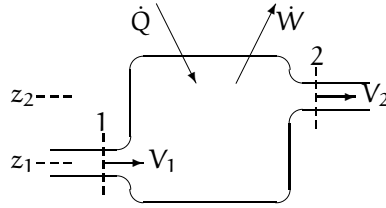


Figure B.1 Figure for analyzing a steady-flow, open system with one inlet and one outlet.

Work, W , done by the system is defined positive, while heat, Q , is accounted as positive when it is added to the system. Using this and neglecting effects of electricity, magnetism, and surface tension, in equation (B.2) the first law of thermodynamics for a steady-flow system with one inlet and one outlet becomes

$$\dot{Q} - \dot{W} = \dot{m} \left(h_2 - h_1 + \frac{V_2^2 - V_1^2}{2} + g(z_2 - z_1) \right)$$

where h denotes enthalpy and z height from a (properly chosen) reference point. Figure B.1 is used for analysis of such a system. Dividing this equation by the mass rate of flow, and neglecting the heat transfer with the surroundings and the change in potential energy, the first law equation on a unit mass basis becomes:

$$-w = \underbrace{h_2 - h_1}_{\text{Static}} + \underbrace{\frac{V_2^2 - V_1^2}{2}}_{\text{Dynamic}} = \underbrace{h_{02} - h_{01}}_{\text{Total}}$$

That is the work done per unit mass equals the change in total, or stagnation, enthalpy, which is the sum of the static and dynamic part.

When performing measurements one must make sure to know if static, dynamic or total temperature is considered. For example if a fluid flows along a straight wall the static pressure can be measured by means of a small opening in the wall as the velocity component, and thus the dynamic pressure, equals zero along the wall. Total temperature can be measured with a probe placed so that the sensor is in contact with only the fluid that has been brought to rest isentropically.

B.2.3 Thermodynamic Properties

In this section some properties that are used in this thesis are presented.

The pressure p , specific volume v , and absolute temperature T of an ideal gas are related by the ideal gas law

$$pv = RT \quad (\text{B.3})$$

The gas constant is different for each gas is given by

$$R = \frac{\tilde{R}}{M}$$

where $\tilde{R} = 8.31441 \frac{\text{kJ}}{\text{kmolK}}$ and M is the molar weight of the gas $\frac{\text{kg}}{\text{kmol}}$.

It follows from equation (B.3) that the internal energy u of an ideal gas is a function of temperature only:

$$u = u(T)$$

Since the enthalpy h is given by $u + pv$, it follows also that

$$h = h(T)$$

The specific heats at constant volume and constant pressure of an ideal gas, c_v and c_p , respectively, are defined by

$$c_v = \left(\frac{\delta u}{\delta T} \right)_v = \frac{du}{dT}$$

$$c_p = \left(\frac{\delta h}{\delta T} \right)_p = \frac{dh}{dT}$$

From equation (B.3) it follows that

$$c_p - c_v = R$$

The ratio of the two specific heats, γ , is a useful quantity:

$$\gamma = \frac{c_p}{c_v}$$

For a perfect gas the heat capacity is a function of T only, however in limited temperature intervals it can be considered to be constant. This is an additional restrictive assumption that is often used to simplify calculations, but is not a necessary part of the ideal gas relationships.